Heavy Flavour Results from the ATLAS Experiment

-> Yes, ATLAS also does Flavour Physics!

Dominic Jones on behalf of the ATLAS Collaboration

Vietnam Flavour Physics Conference 2025

Introduction

- This talk will cover two recent heavy flavour results from the ATLAS Experiment :
    - Precision measurement of the B^0 lifetime – EPJC 85 (2025) 736
    - Differential Cross-section measurements of $D^{\pm}$ and $D_s^{\pm}$ production - JHEP 07 (2025) 86
- ATLAS is a **hermetic, general purpose detector** designed to measure a wide range of particle physics phenomena at the LHC
- Most relevant parts of ATLAS for B-physics measurements are the Inner Detector (ID) and Muon Spectrometer (MS)
    - ID allows **precise reconstruction of charged tracks** for $|\eta| < 2.5$
    - MS further improves **muon reconstruction and triggering** on muons, covers $|\eta| < 2.7$

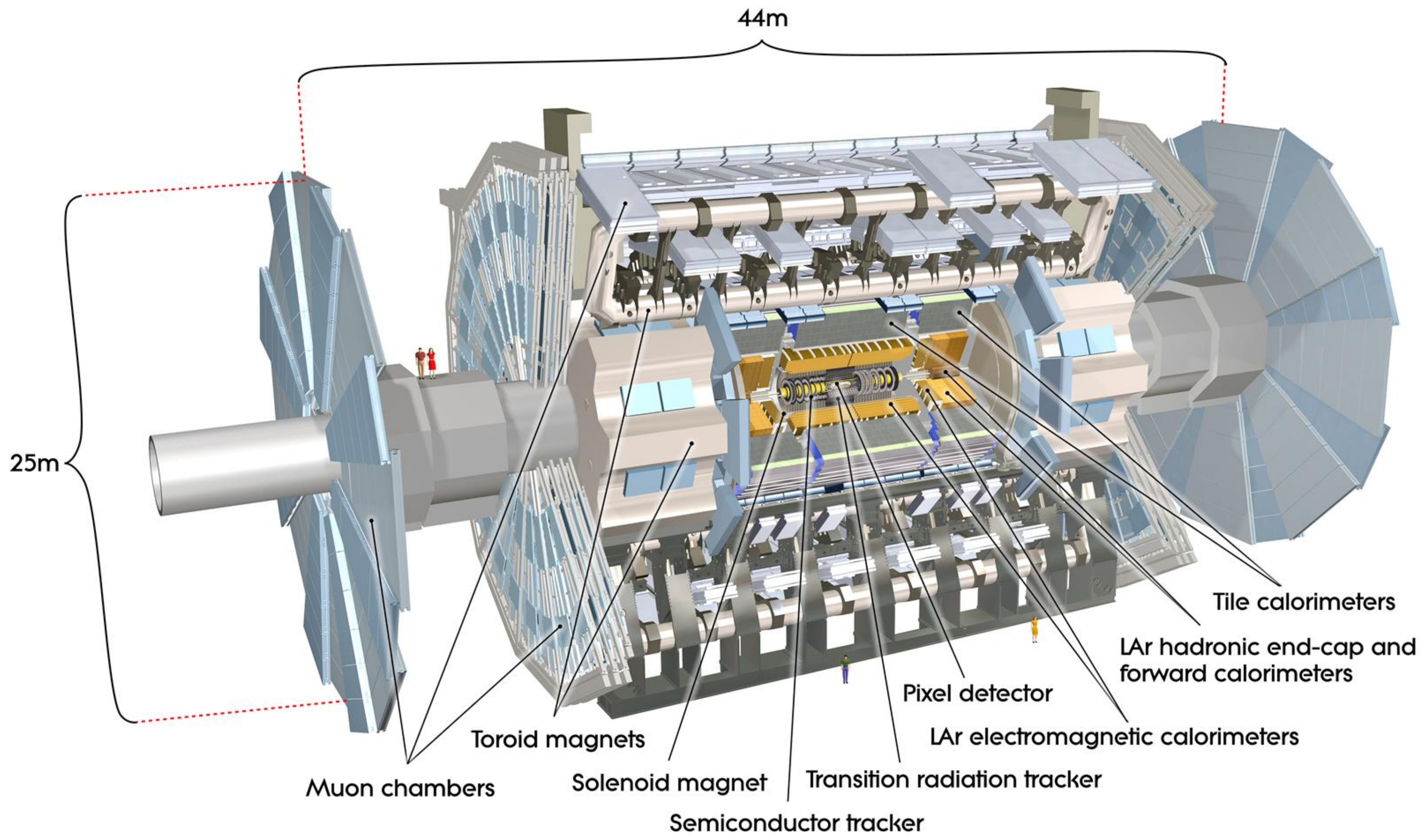

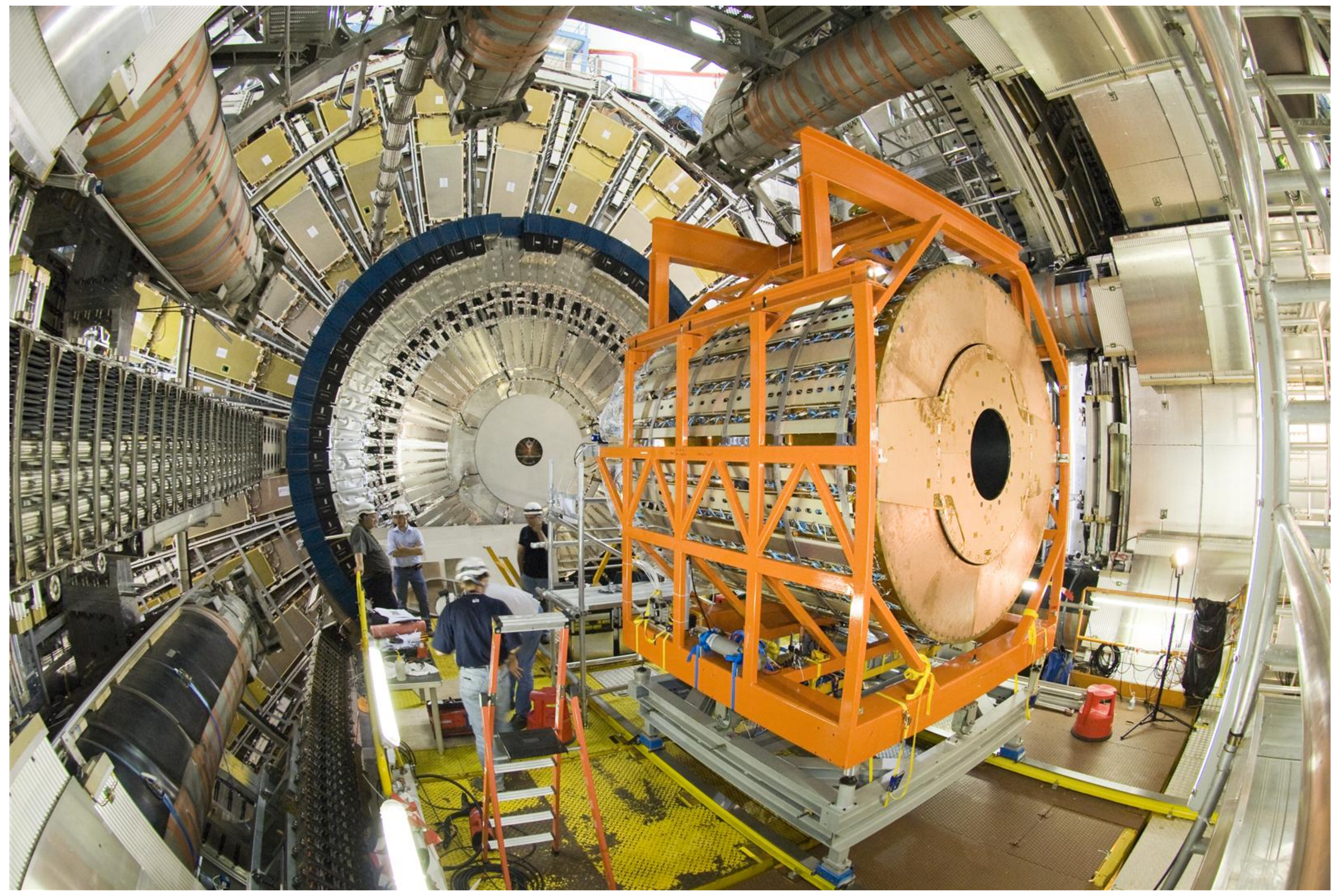

Inner Detector

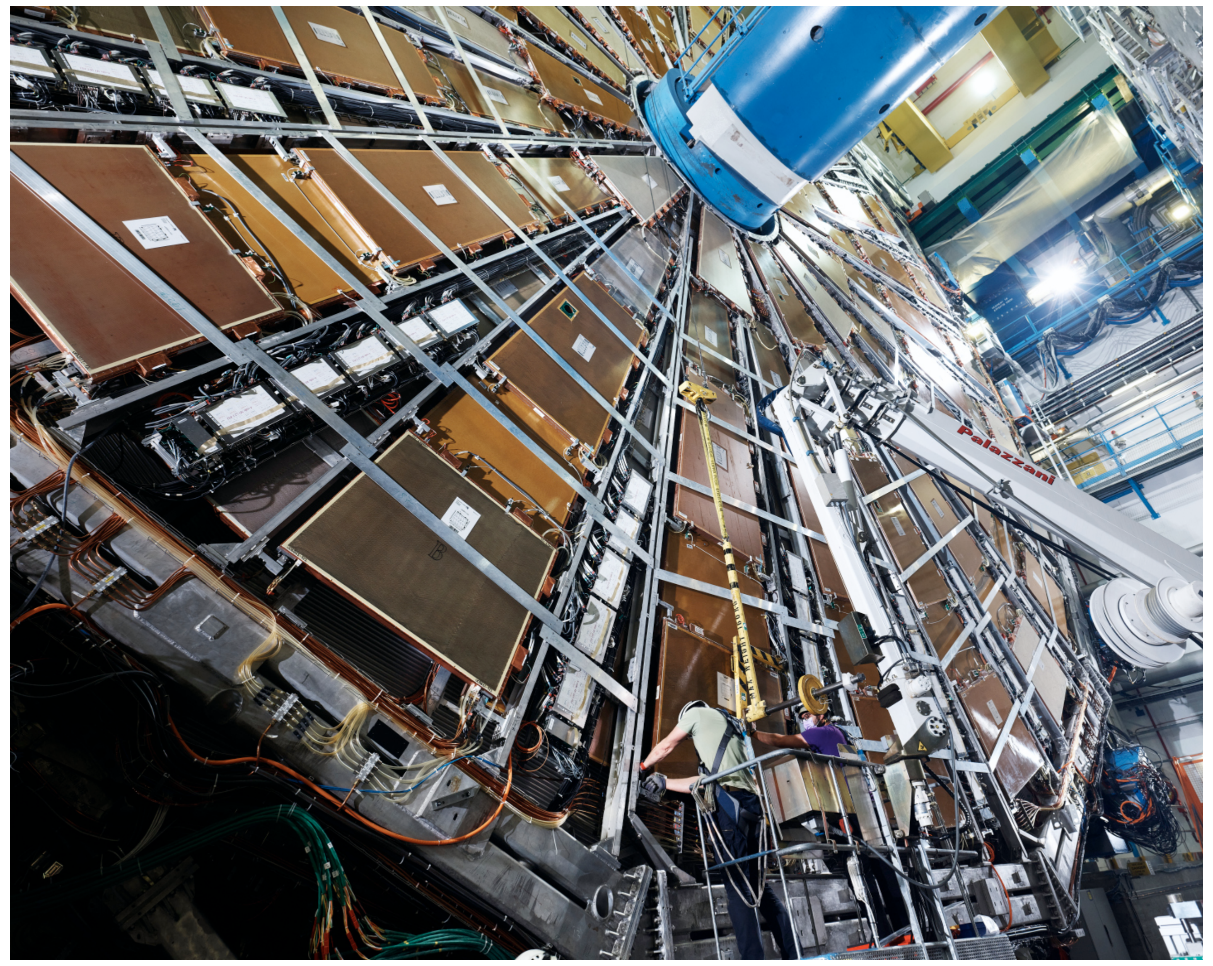

Muon Spectrometer

Precision Measurement of B^0 Lifetime

EPJC 85 (2025) 736

Precision Measurement of B^0 Lifetime

- Studies of B-hadron lifetimes **test our understanding of the Weak Interaction** and can be used to test New Physics models
- Measured Lifetime can be converted to decay width, Γ_d, which can be compared with theoretical predictions from the **Heavy Quark Expansion (HQE)**
- The new result by ATLAS is the **most precise measurement** to date of the B^0 lifetime
- See CERN Courier article (p. 15) and LHC-seminar

ATLAS

A new record for precision on B-meson lifetimes

As direct searches for physics beyond the Standard Model continue to push frontiers at the LHC, the b-hadron physics sector remains a crucial source of insight for testing established theoretical models.

The ATLAS collaboration recently published a new measurement of the B^0 lifetime using $B^0 \to J/\psi K^{*0}$ decays from the entire Run-2 dataset it has recorded at 13 TeV. The result improves the precision of previous world-leading measurements by the CMS and LHCb collaborations by a factor of two.

Studies of b-hadron lifetimes probe our understanding of the weak interaction. The lifetimes of b-hadrons can be systematically computed within the heavy-quark expansion (HQE) framework, where b-hadron observables are expressed as a perturbative expansion in inverse powers of the b-quark mass.

ATLAS measures the "effective" B^0 lifetime, which represents the average decay time incorporating effects from mixing and CP contributions, as $\tau(B^0) = 1.5053 \pm 0.0012\,(\text{stat.}) \pm 0.0035\,(\text{syst.})$ ps. The result is consistent with previous measurements published by ATLAS and other experiments, as summarised in figure 1. It also aligns with theoretical predictions from HQE and lattice QCD, as well as with the experimental world average.

The analysis benefitted from the large Run-2 dataset and a refined trigger selection, enabling the collection of an extensive sample of 2.5 million $B^0 \to J/\psi K^{*0}$ decays. Events with a J/ψ meson decaying into two muons with sufficient transverse momentum are cleanly identified in the ATLAS Muon Spectrometer by the first-level hardware trigger. In the next-level software trigger, exploiting the full detector information, these muons are then combined with two tracks measured by the Inner Detector, ensuring they originate from the same vertex.

The B^0-meson lifetime is determined through a two-dimensional unbinned maximum-likelihood fit, utilising the measured B^0-candidate mass and decay time, and accounting for both signal and background components. The limited hadronic particle-identification capability of ATLAS requires careful modelling of the significant backgrounds from other processes that produce J/ψ mesons. The sensitivity of the fit is increased by estimating the uncertainty of the decay-time measurement provided by the ATLAS tracking and vertexing algorithms on a per-candidate basis. The resulting lifetime measurement is limited by systematic uncertainties, with the largest contributions arising from the correlation between B^0 mass and lifetime, and ambiguities in modelling the mass distribution.

ATLAS combined its measurement with the average decay width (Γ_s) of the light and heavy B_s-meson mass eigenstates, also measured by ATLAS, to determine the ratio of decay widths as $\Gamma_d/\Gamma_s = 0.9905 \pm 0.0022\,(\text{stat.}) \pm 0.0036\,(\text{syst.}) \pm 0.0057\,(\text{ext.})$. The result is consistent with unity and provides a stringent test of QCD predictions, which also support a value near unity.

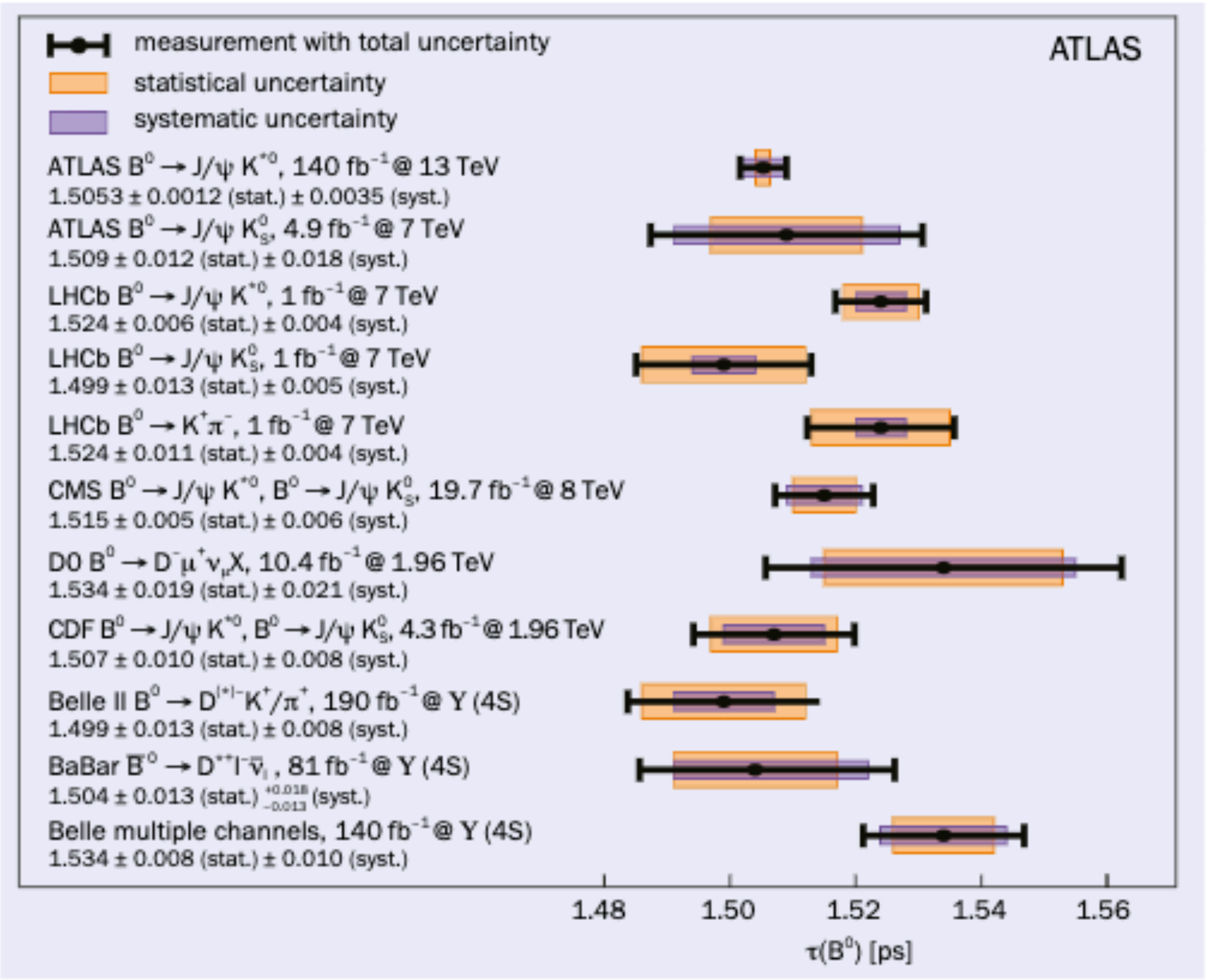

ATLAS Collab. 2024 arXiv:2411.09962

Fig. 1. *A comparison of the current ATLAS result for the B^0 lifetime with the previous ATLAS result in the $B^0 \to J/\psi K^0_S$ channel, and with those from other experiments.*

Further reading

ATLAS Collab. 2024 arXiv:2411.09962.
ATLAS Collab. 2021 *Eur. Phys. J. C* **81** 342.

Theory Prediction

- Decay width, Γ_d, can be computed using the **Heavy Quark Expansion (HQE)** framework:

$$\Gamma(\mathscr{B}_q) = \Gamma_3 + \delta\Gamma(\mathscr{B}_q)$$

leading

subleading

Free b-quark decay:

+ free of non-perturbative uncertainties

0 Looks like the muon decay

$$\Gamma_3 \propto \frac{G_F^2 m_b^5}{192\pi^3} V_{cb}^2$$

- Quark masses are difficult to define, huge dependence on definition can be reduced by higher order **perturbative corrections**

Power-suppressed terms on the HQE:

+ suppressed with at least 2 powers of $1/m_b \Rightarrow$ small

0 Individual contributions are products of **perturbative** Wilson coefficients and **non-perturbative matrix elements** (determined with lattice-QCD, sum rules and/or from fits of experimental data of inclusive semi-leptonic decays - V_{cb})

- Relatively large uncertainties on Γ_3 term, prediction for $\Gamma_d = 0.63^{+0.11}_{-0.07}$ ps^{-1} (Lenz et al.)

- Note however these large uncertainties cancel in ratios of Γ for different hadrons

Analysis Strategy

- Uses the $B^0 \to K^{*0} J/\psi$ with $K^{*0} \to K^{\pm}\pi^{\mp}$ and $J/\psi \to \mu^+\mu^-$ channel
- Analyses the $139\ \mathrm{fb}^{-1}$ of data collected between **2015-2018** by the ATLAS Experiment
- **Trigger on $J/\psi(\to \mu\mu)$,** with muon thresholds between 11 GeV and 4 GeV (lower threshold at end of LHC fills) **and two opposite sign tracks**
- Reconstruct B^0 candidates using ID + MS information for Muons and matching ID tracks for Kaons and Pions (no general Kaon/Pion PID in ATLAS)
- Fit to **common vertices** in turn for each of the K^{*0}, J/ψ and B^0
- **Minimal selection requirements** so as not to bias the decay time distributions

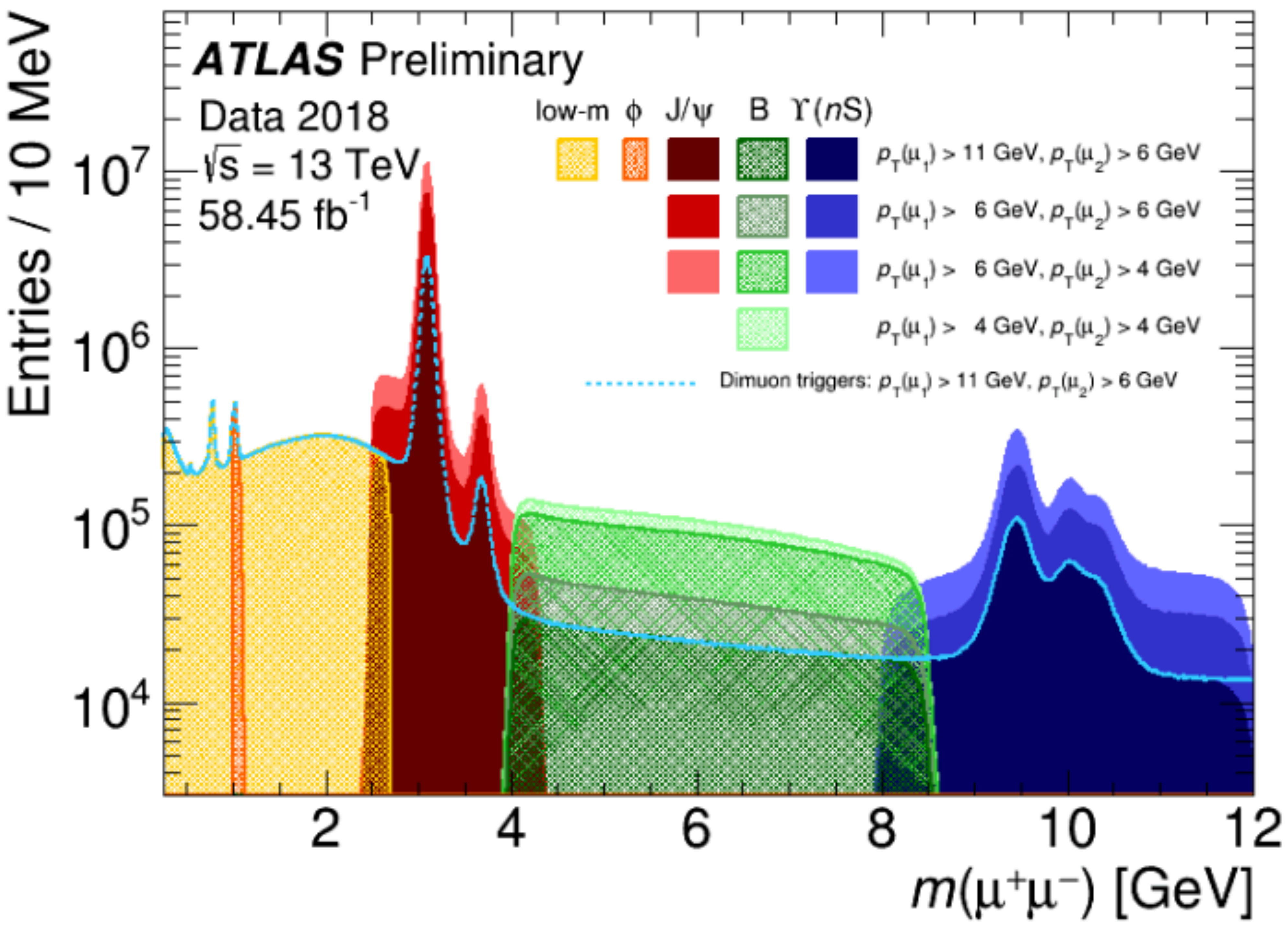

Invariant mass distribution of offline selected dimuon candidates, colours indicate trigger passed

The proper decay time for each candidate is determined as

$$t = \frac{L_{xy} m_B}{p_{T_B}}$$

where L_{xy} is the transverse decay length

Analysis Strategy (cont.)

B^0 Lifetime is extracted from a **2D maximum likelihood fit** in the B-candidate invariant mass and decay time

Mass PDFs

Decay time PDFs

$$\ln L = \sum_{i=1}^{N} w(t_i) \ln[f_{\rm sig} \mathcal{M}_{\rm sig}(m_i) \mathcal{T}_{\rm sig}(t_i, \sigma_{t_i}, p_{{\rm T}_i}) + (1 - f_{\rm sig}) \mathcal{M}_{\rm bkg}(m_i) \mathcal{T}_{\rm bkg}(t_i, \sigma_{t_i}, p_{{\rm T}_i})]$$

Signal fraction

Decay time

Decay time uncertainty

Weight to account for selection efficiency, given by inverse of time efficiency functions

Error function

$$1/w_i(t_i) = p_0 \cdot [1 - p_1 \cdot (\mathrm{Erf}((t_i - p_3)/p_2) + 1)]$$

Parameters determined from fits to simulation

Invariant Mass Distribution

- Signal is modelled by **Johnson S_U -distribution**
- Background modelled by **polynomial + sigmoid** function
  - Sigmoid helps to describe contribution from partially reconstructed B-mesons at lower mass values
- $2{,}450{,}500 \pm 2400$ $B^0 \to J/\psi K^{*0}$ **signal candidates**

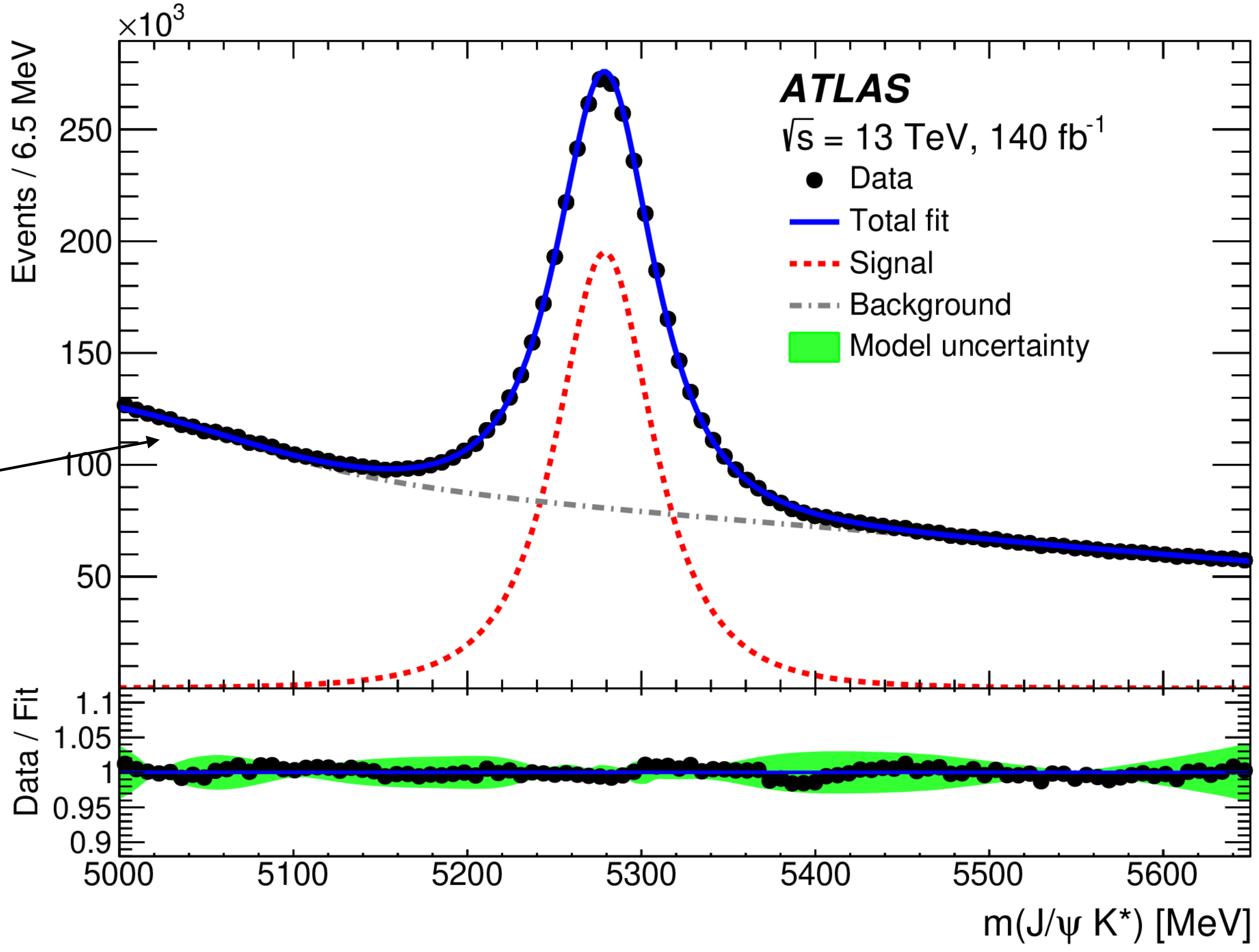

Decay Time Distribution

Decay time PDF split into two parts:

$$\mathcal{T}_j(t_i, \sigma_{t_i}, p_{\mathrm{T}_i}) = P_j(t_i|\sigma_{t_i}, p_{\mathrm{T}_i}) \cdot C_j(\sigma_{t_i}, p_{\mathrm{T}_i})$$

Functions describing the **decay time distribution**:

- Signal decay time modelled as an **exponential convolved with resolution function**, which is the sum of three Gaussian distributions
- Background split into '**prompt**' and **combinatorial** components
  - Prompt part modelled by resolution function
  - Combinatorial by the sum of three exponentials convolved with resolution function

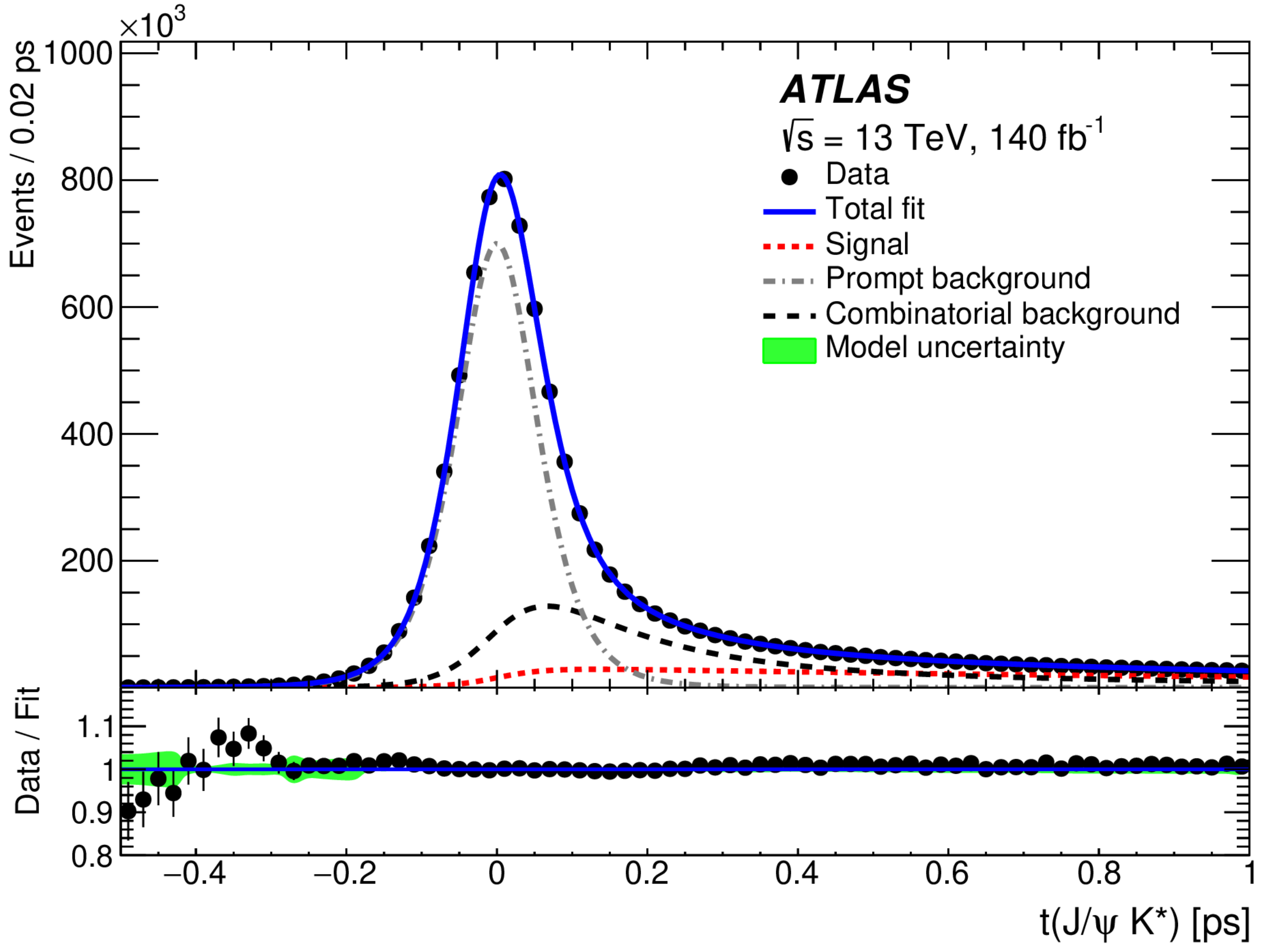

Probability terms - 2D distributions, account for the differences between signal and background for per candidate σ_{t_i} and p_{T_i} values (see G. Punzi)

- **Distributions for σ_{t_i} extracted from data** via the sPlot method, using invariant mass distribution as control variable

Decay Time Distribution

Decay time PDF split into two parts:

$$\mathcal{T}_j(t_i, \sigma_{t_i}, p_{\mathrm{T}_i}) = P_j(t_i|\sigma_{t_i}, p_{\mathrm{T}_i}) \cdot C_j(\sigma_{t_i}, p_{\mathrm{T}_i})$$

Functions describing the **decay time distribution**:

- Signal decay time modelled as an **exponential convolved with resolution function**, which is the sum of three Gaussian distributions
- Background split into '**prompt**' and **combinatorial** components
  - Prompt part modelled by resolution function
  - Combinatorial by the sum of three exponentials convolved with resolution function

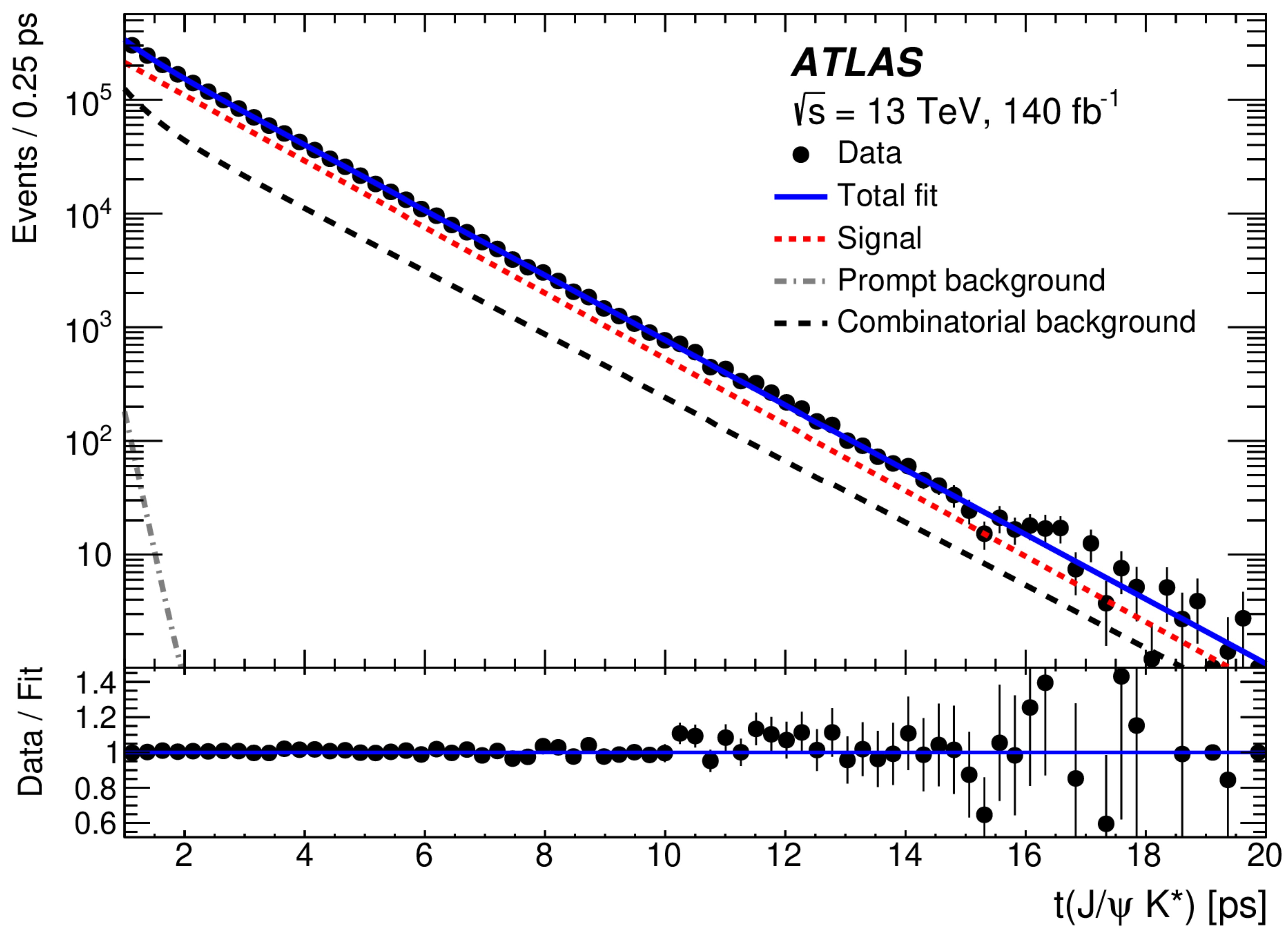

Probability terms - 2D distributions, account for the differences between signal and background for per candidate σ_{t_i} and p_{T_i} values (see G. Punzi)

- **Distributions for σ_{t_i} extracted from data** via the sPlot method, using invariant mass distribution as control variable

Systematic Uncertainties

ID misalignment effectively removed by constraining mass of J/ψ candidates to PDG value - assess uncertainty by removing constraint. Also assess momentum scale bias effecting low p_T hadrons

Source of uncertainty	Systematic uncertainty [ps]
ID alignment	0.00108
Choice of mass window	0.00104
Time efficiency	0.00135
Best-candidate selection	0.00041
Mass fit model	0.00152
Mass-time correlation	0.00229
Proper decay time fit model	0.00010
Conditional probability model	0.00070
Fit model test with pseudo-experiments	0.00002
Total	0.0035

Test **alternative time efficiency functions**

Studied using signal MC and sideband data

Test **alternative PDFs**

Test different choices of binning and smoothing methods

Test **alternative PDFs** for signal and background components and inclusion of additional processes with misidentified for missing tracks

Statistical uncertainty: 0.0012 ps

Results

Measure $\tau_{B^0} = 1.5053 \pm 0.0012(\textbf{stat.}) \pm 0.0035(\textbf{syst.})\textbf{ps}$

- Most precise measurement to date, differs from 2024 PDG World average by 2.1σ

Using HFLAV values, convert this into average B_d decay width of:
$\Gamma_d = 0.6639 \pm 0.0005(\textbf{stat.}) \pm 0.0016(\textbf{syst.}) \pm 0.0038(\textbf{ext.})\textbf{ps}^{-1}$

- Agrees with HQE theory prediction of $0.63^{+0.11}_{-0.07}$ ps^{-1}

Additionally, use previous ATLAS study of $B_s \to J/\psi\phi$ decays in which Γ_s was measured to compute the ratio
$$\frac{\Gamma_d}{\Gamma_s} = 0.9905 \pm 0.22(\textbf{stat.}) \pm 0.0036(\textbf{syst.}) \pm 0.0057(\textbf{ext.})$$

- Agrees with HQE (1.003 ± 0.006) and lattice QCD (1.00 ± 0.02) predictions

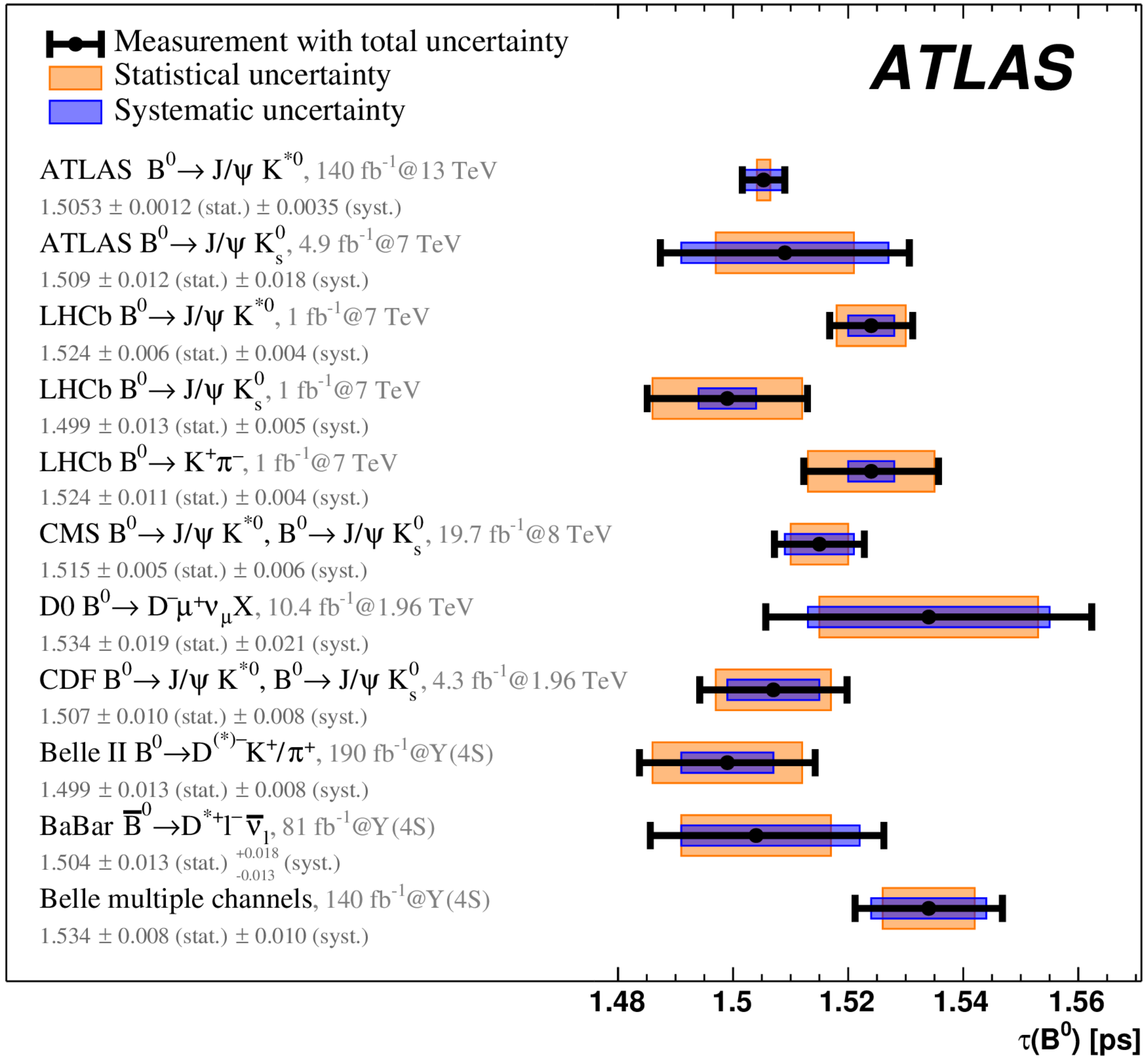

$D^{\pm}$ and $D_s^{\pm}$ Production cross-sections

JHEP 07 (2025) 86

$D^{\pm}$ and $D_s^{\pm}$ Production cross-sections

- Measuring the production of heavy hadrons at the LHC is important for **testing QCD**
- Current **theoretical uncertainties are large** due to quark masses being close to energy scale of hard scatter
- **New result** provides measurement of $D^{\pm}$ and $D_s^{\pm}$ inclusive and differential cross-sections in p_T and η, for **first time in ATLAS at $\sqrt{s} = 13$ TeV**
- Measurements compared with predictions from **GM-VFNS** and **FONLL** models (setup described in previous ATLAS result)

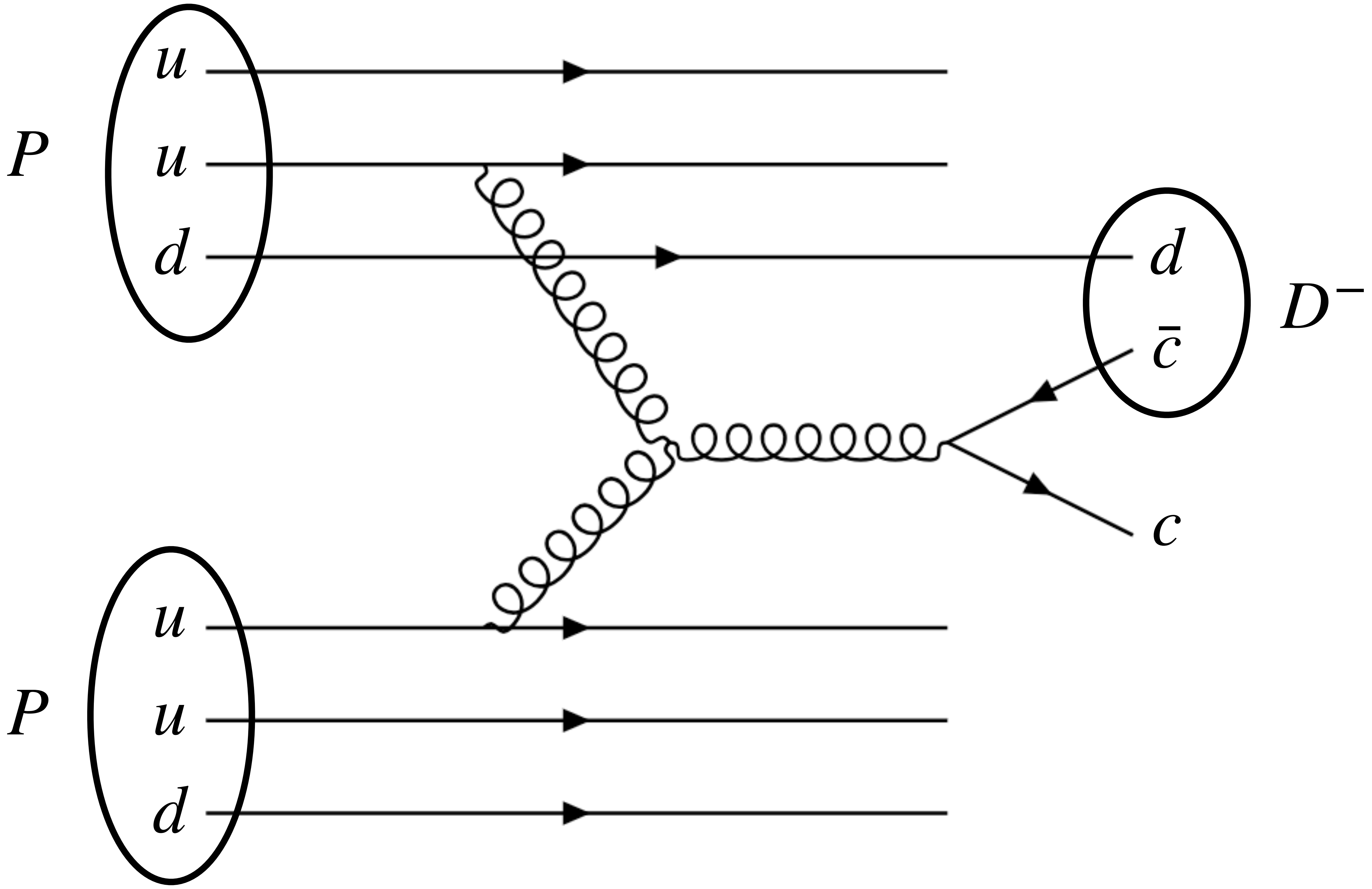

GM-VFNS = General-mass variable-flavour-number scheme

FONLL = Fixed-order next-to-leading-logarithm

Analysis Strategy

- Using the $D^{\pm}_{(s)} \to \phi\pi^{\pm}$ decay channel with $\phi \to \mu^{+}\mu^{-}$ and the data collected between **2016 and 2018**
- **Trigger using the muons** from $\phi \to \mu^{+}\mu^{-}$, p_T thresholds of at least 11-6 (6) GeV on the leading (sub-leading) muon
- **Reconstruct the decay vertex** using Inner Detector (ID) + Muon Spectrometer info for the muons and assign additional ID track to the Pion
- Separation between primary and secondary vertices used to reject backgrounds
- Selection **prioritises prompt $D^{\pm}_{(s)}$ production** but both prompt and non-prompt $D^{\pm}_{(s)}$ mesons are considered as signal

Selection	
Muon objects	Two muons satisfying the *Loose* working point
Track object	One track satisfying the *Loose* working point
Transverse momentum	$p_{\mathrm{T}}^{\mu} > 6\,\mathrm{GeV}$, $p_{\mathrm{T}}^{\pi} > 1\,\mathrm{GeV}$
Opposite charge muons	$Q_{\mu_1} \times Q_{\mu_2} = -1$
Total charge	$\lvert Q_{\mu\mu\pi}\rvert = 1$
Di-muon invariant mass	$\lvert m_{\mu\mu} - m_{\phi}\rvert < \delta m(\lvert\eta\rvert)$
L_{xy} significance	$\mathrm{Sig}(L_{xy}) > 3$
a^0_{xy} significance	$\lvert\mathrm{Sig}(a^0_{xy})\rvert < 4$
Vertex p-value	$\log(p_0^{\mathrm{vertex}}) > -0.8$
Highest vertex p-value	The vertex with $\mathrm{Max}(p_0^{\mathrm{vertex}})$ in the event

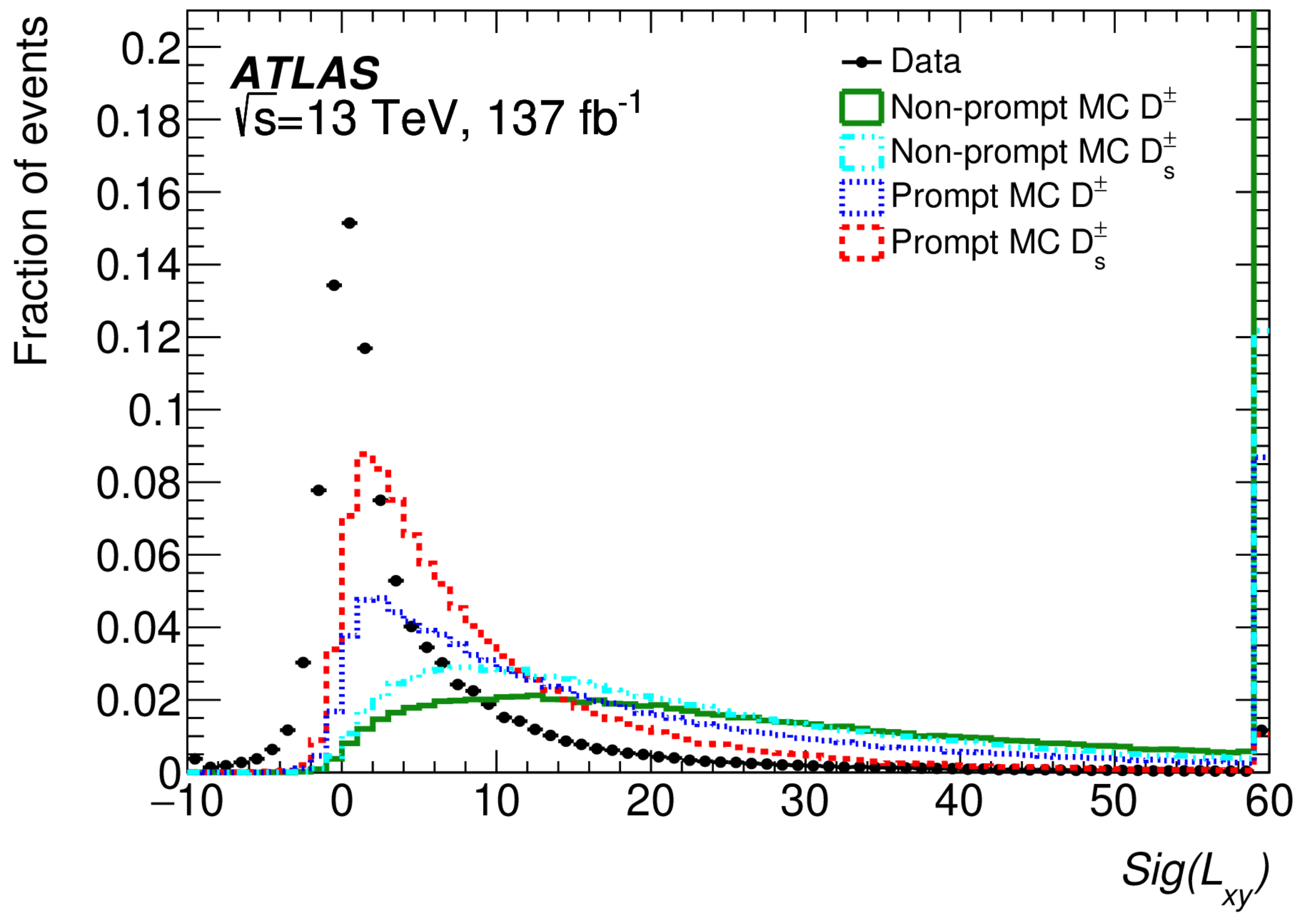

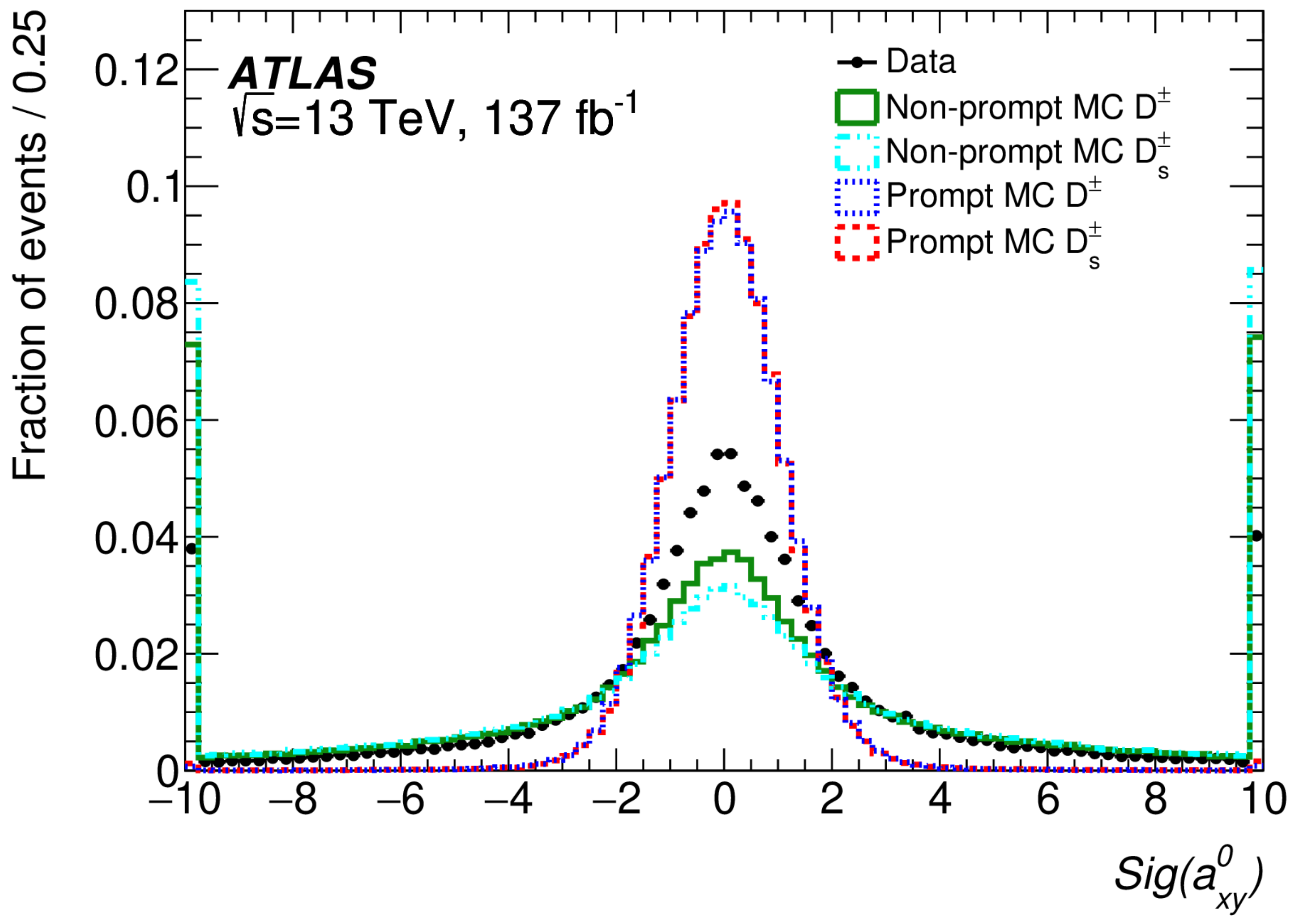

$L_{xy} = |\vec{L}_T|\cos(\theta_{xy})$, $a^0_{xy} = |\vec{L}_T|\sin(\theta_{xy})$ where $\vec{L}$ is the vector connecting the PV and SV in transverse plane and θ_{xy} is the angle between $\vec{L}_T$ and the p_T of the $\mu\mu\pi$ system

Analysis Strategy

- **Signal yields** are extracted from fits to the $\mu\mu\pi$ invariant mass in **bins of p_T and η**
- Mass fit model consists of **Voigtian** (Breit-Wigner * Gaussian) distributions for each of the $D^{\pm}$ and $D_s^{\pm}$ signals and a **quadratic exponential** distribution for the **background**
- Monte Carlo (MC) simulation is used to compute the **relative efficiency per bin**
  - MC **p_T and η distributions are corrected** to match signal shape from data
- Shapes in general extracted from fits to data but simultaneous fits with MC used for some bins to improve fit stability

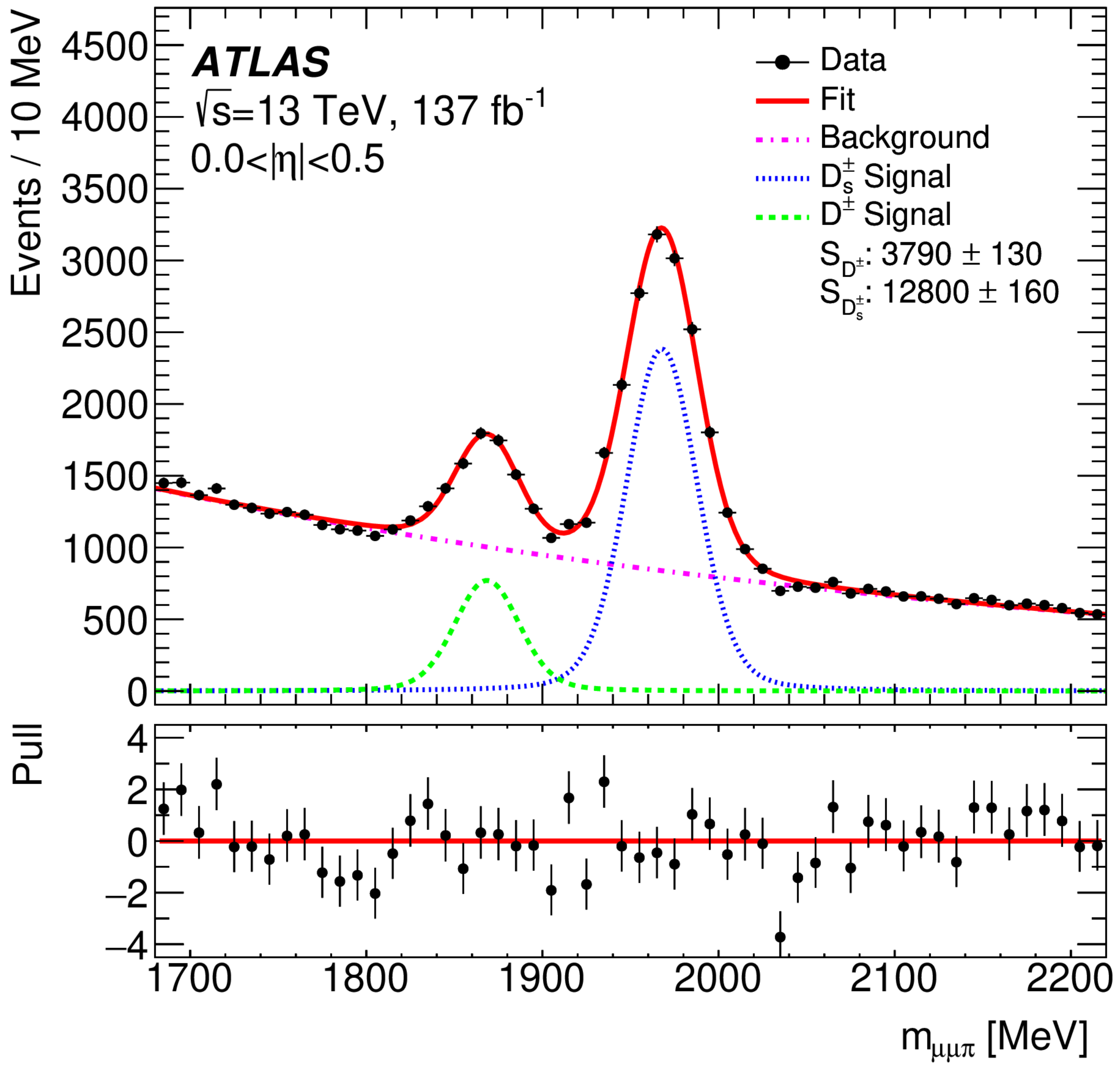

Example Invariant Mass fit for $0 < |\eta| < 0.5$

Non-prompt Fraction Correction

Fraction of prompt to non-prompt $D^{\pm}_{(s)}$ production in MC simulations is **corrected** from fits to the proper decay time:

- **Invariant mass fits** are performed in **bins of lifetime** from which the total prompt + non prompt yield is extracted
- **Templates** for the prompt and non-prompt lifetime distributions **derived from MC simulation** are then fit to the data to extract the non-prompt fraction
- Procedure is applied separately to $D^{\pm}$ and $D_s^{\pm}$ in **three bins of p_T** ([12, 20, 30, 100] GeV)

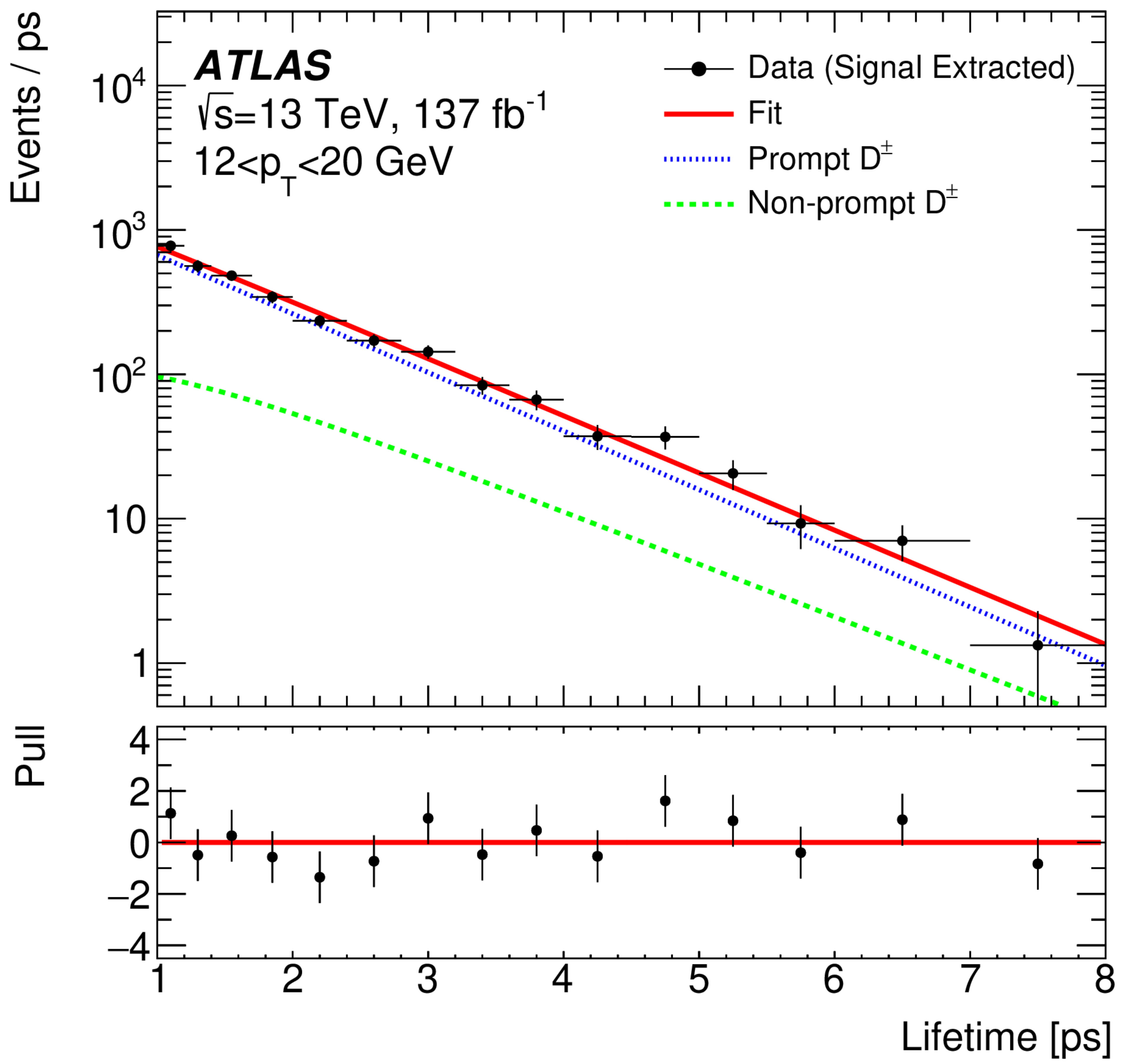

$$P_{b\bar{b}}(\tau) = \mathrm{Exp}(\tau; \tau_D^{b\bar{b}}) * \mathrm{Exp}(\tau; \tau_B^{b\bar{b}}) * \mathrm{Gauss}(\tau; \mu^{b\bar{b}}, \sigma_{\mathrm{res}}^{b\bar{b}}) * \mathrm{Erf}(\tau; \tau_{\text{turn-on}}^{b\bar{b}}, \beta^{b\bar{b}}),$$
$$P_{c\bar{c}}(\tau) = \mathrm{Exp}(\tau; \tau_D^{c\bar{c}}) * \mathrm{Gauss}(\tau; \mu^{c\bar{c}}, \sigma_{\mathrm{res}}^{c\bar{c}}) * \mathrm{Erf}(\tau; \tau_{\text{turn-on}}^{c\bar{c}}, \beta^{c\bar{c}}).$$

Systematic Uncertainties

- Several sources of uncertainty are considered:
  - **Detector effects** (muon and track reconstruction, trigger efficiencies etc.)
  - Use of different signal and background **fit models**, and contributions from **partially reconstructed D-meson decays**
  - Uncertainties from **prompt/non-prompt corrections** are propagated into the final result
  - External Branching Ratio $\mathscr{B}(D^{\pm}_{(s)} \to \phi(\mu\mu)\pi^{\pm})$

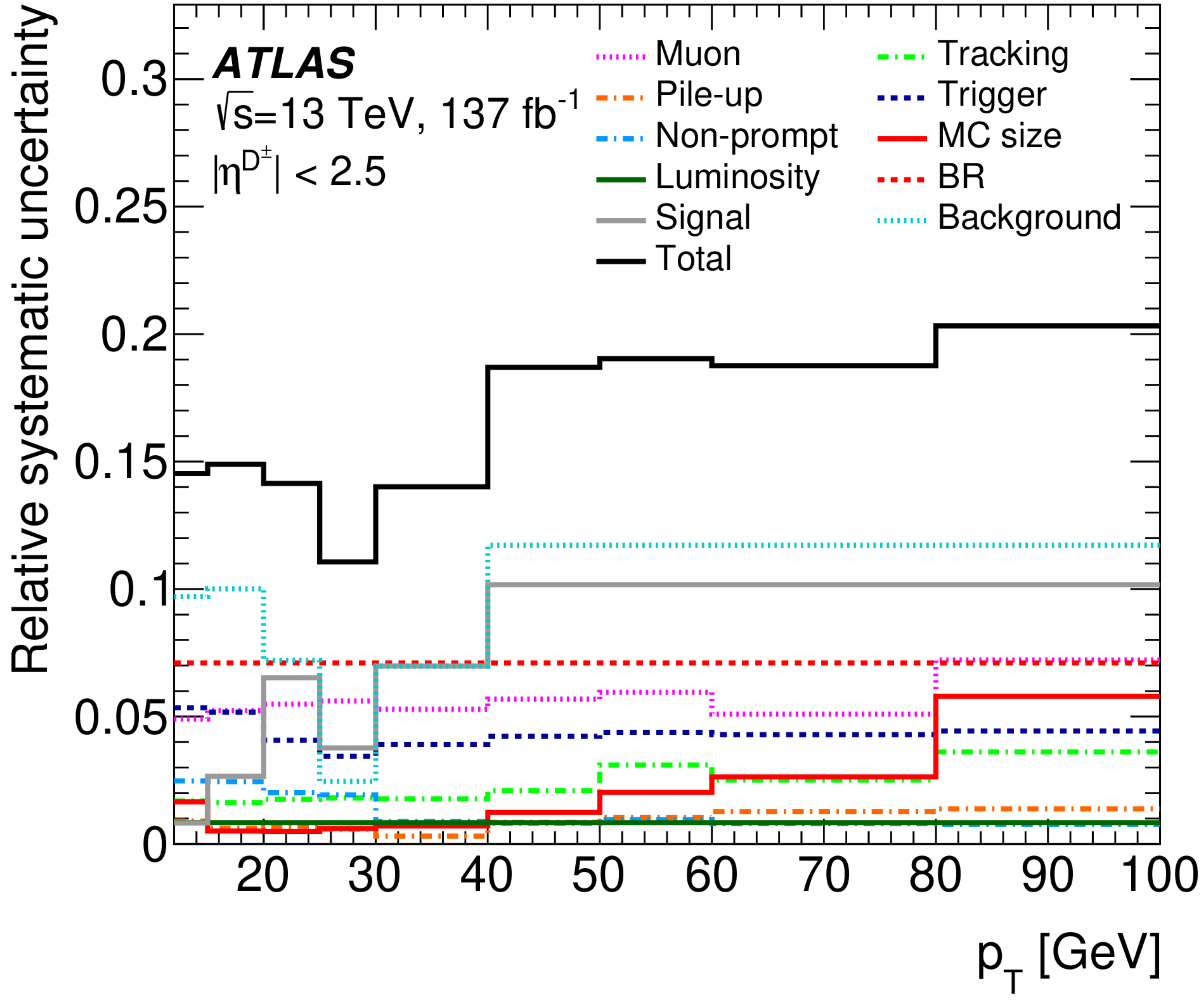

$D^{\pm}$ uncertainty breakdown as a function of p_T

Results: Inclusive Cross-sections

- Inclusive cross-sections are provided for **three different p_T ranges**

Fiducial volume	$D^{\pm}$ inclusive fiducial cross-section at $\sqrt{s}$ = 13 TeV [nb] ATLAS $\sigma \pm \delta_{\text{stat}} \pm \delta_{\text{syst}} \pm \delta_{\text{BR}}$
$12 < p_{\text{T}} < 100$ GeV, $\lvert\eta\rvert < 2.5$	10 800 ± 900 ± 1 300 ± 800
$15 < p_{\text{T}} < 100$ GeV, $\lvert\eta\rvert < 2.5$	5 430 ± 550 ± 680 ± 390
$20 < p_{\text{T}} < 100$ GeV, $\lvert\eta\rvert < 2.5$	1 930 ± 160 ± 220 ± 140

$D^{\pm}$

Fiducial volume	$D_s^{\pm}$ inclusive fiducial cross-section at $\sqrt{s}$ = 13 TeV [nb] ATLAS $\sigma \pm \delta_{\text{stat}} \pm \delta_{\text{syst}} \pm \delta_{\text{BR}}$
$12 < p_{\text{T}} < 100$ GeV, $\lvert\eta\rvert < 2.5$	5 000 ± 360 ± 470 ± 360
$15 < p_{\text{T}} < 100$ GeV, $\lvert\eta\rvert < 2.5$	2 440 ± 190 ± 220 ± 180
$20 < p_{\text{T}} < 100$ GeV, $\lvert\eta\rvert < 2.5$	920 ± 60 ± 80 ± 70

$D_s^{\pm}$

Results: Inclusive Cross-sections

- Inclusive cross-sections are provided for **three different p_T ranges**
- **Good agreement** with **GM-VFNS** and **FONLL** models for both $D^{\pm}$ and $D_s^{\pm}$,
- New measurements have smaller uncertainties than predictions

$D^{\pm}$ inclusive fiducial cross-section at $\sqrt{s} = 13$ TeV [nb]

Fiducial volume	ATLAS $\sigma \pm \delta_{\text{stat}} \pm \delta_{\text{syst}} \pm \delta_{\text{BR}}$	GM-VFNS $\sigma \pm \delta_{\text{theory}}$	FONLL $\sigma \pm \delta_{\text{theory}}$
$12 < p_{\text{T}} < 100$ GeV, $\|\eta\| < 2.5$	$10\,800 \pm 900 \pm 1\,300 \pm 800$	$14\,100^{+2\,900}_{-2\,300}$	$10\,200^{+2\,300}_{-1\,700}$
$15 < p_{\text{T}} < 100$ GeV, $\|\eta\| < 2.5$	$5\,430 \pm 550 \pm 680 \pm 390$	$6\,800^{+1\,200}_{-1\,000}$	$4\,730^{+900}_{-700}$
$20 < p_{\text{T}} < 100$ GeV, $\|\eta\| < 2.5$	$1\,930 \pm 160 \pm 220 \pm 140$	$2\,480^{+350}_{-330}$	$1\,670^{+260}_{-220}$

$D_s^{\pm}$ inclusive fiducial cross-section at $\sqrt{s} = 13$ TeV [nb]

Fiducial volume	ATLAS $\sigma \pm \delta_{\text{stat}} \pm \delta_{\text{syst}} \pm \delta_{\text{BR}}$	GM-VFNS $\sigma \pm \delta_{\text{theory}}$
$12 < p_{\text{T}} < 100$ GeV, $\|\eta\| < 2.5$	$5\,000 \pm 360 \pm 470 \pm 360$	$5\,900^{+1\,200}_{-1\,000}$
$15 < p_{\text{T}} < 100$ GeV, $\|\eta\| < 2.5$	$2\,440 \pm 190 \pm 220 \pm 180$	$2\,880^{+510}_{-440}$
$20 < p_{\text{T}} < 100$ GeV, $\|\eta\| < 2.5$	$920 \pm 60 \pm 80 \pm 70$	$1\,070^{+150}_{-140}$

$D^{\pm}$

$D_s^{\pm}$

Results: Differential Cross-sections

For $D^{\pm}$:

- Good agreement with both **GM-VFNS** and **FONLL** seen at low p_T and in η
- High p_T, **GM-VFNS** tends to over-predict while **FONLL** still has good agreement

For $D_s^{\pm}$:

- Only **GM-VFNS** available - again gives good agreement at low p_T and in η, larger deviation at high p_T

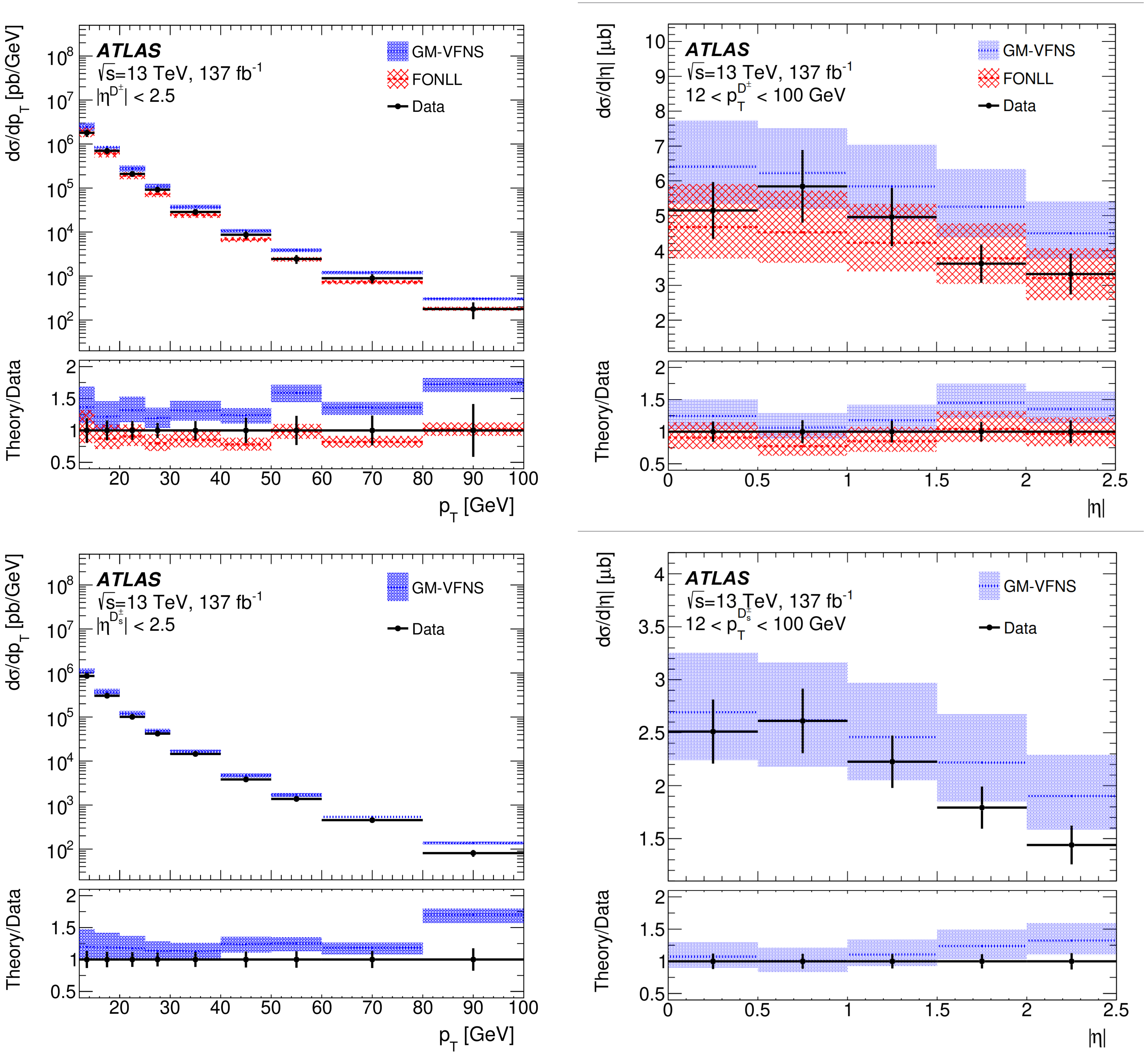

$D^{\pm}$

$D_s^{\pm}$

Comparison with ATLAS $\sqrt{s} = 7$ TeV Result

- Compared to previous ATLAS result at $\sqrt{s} = 7$ TeV which used 2010 data

	$D^{\pm}$ inclusive fiducial cross-section [nb]
	ATLAS
	$\sigma \pm \delta_{\text{total}}$
$\sqrt{s} = 13$ TeV	$1\,690 \pm 270$
$\sqrt{s} = 7$ TeV	888 ± 97

	$D_s^{\pm}$ inclusive fiducial cross-section [nb]
	ATLAS
	$\sigma \pm \delta_{\text{total}}$
$\sqrt{s} = 13$ TeV	810 ± 100
$\sqrt{s} = 7$ TeV	510 ± 100

Comparison with ATLAS $\sqrt{s} = 7$ TeV Result

- Compared to previous ATLAS result at $\sqrt{s} = 7$ TeV which used 2010 data
- **Ratios between 13 TeV and 7 TeV** cross sections also computed

	$D^{\pm}$ inclusive fiducial cross-section [nb]
	ATLAS
	$\sigma \pm \delta_{\text{total}}$
$\sqrt{s}$ = 13 TeV	1 690 ± 270
$\sqrt{s}$ = 7 TeV	888 ± 97
Ratio (13 TeV/7 TeV)	1.9 ± 0.4

	$D_s^{\pm}$ inclusive fiducial cross-section [nb]
	ATLAS
	$\sigma \pm \delta_{\text{total}}$
$\sqrt{s}$ = 13 TeV	810 ± 100
$\sqrt{s}$ = 7 TeV	510 ± 100
Ratio (13 TeV/7 TeV)	1.6 ± 0.4

Comparison with ATLAS $\sqrt{s} = 7$ TeV Result

- Compared to previous ATLAS result at $\sqrt{s} = 7$ TeV which used 2010 data
- **Ratios between 13 TeV and 7 TeV** cross sections also computed
- Measured **ratios agree with both GM-VFNS and FONLL** predictions, though there is a significant difference between the two models

	$D^{\pm}$ inclusive fiducial cross-section [nb]		
	ATLAS	GM-VFNS	FONLL
	$\sigma \pm \delta_{\text{total}}$	$\sigma \pm \delta_{\text{theory}}$	$\sigma \pm \delta_{\text{theory}}$
$\sqrt{s}$ = 13 TeV	$1\,690 \pm 270$	$2\,200^{+310}_{-290}$	$1\,480^{+230}_{-190}$
$\sqrt{s}$ = 7 TeV	888 ± 97	980^{+120}_{-150}	620^{+100}_{-80}
Ratio (13 TeV/7 TeV)	1.9 ± 0.4	2.24 ± 0.04	2.38 ± 0.01

	$D_s^{\pm}$ inclusive fiducial cross-section [nb]	
	ATLAS	GM-VFNS
	$\sigma \pm \delta_{\text{total}}$	$\sigma \pm \delta_{\text{theory}}$
$\sqrt{s}$ = 13 TeV	810 ± 100	950^{+140}_{-130}
$\sqrt{s}$ = 7 TeV	510 ± 100	470^{+56}_{-69}
Ratio (13 TeV/7 TeV)	1.6 ± 0.4	2.02 ± 0.05

Summary

- Presented two recent Heavy Flavour Measurements from the ATLAS Experiment:
  - Most **precise measurement of the B^0 lifetime** – EPJC 85 (2025) 736
  - First measurement by ATLAS of $D^{\pm}_{(s)}$ **inclusive and differential cross-sections at $\sqrt{s} = 13$ TeV** - JHEP 07 (2025) 86
- Both results illustrate the ATLAS experiments capability to make **interesting** and **important flavour physics measurements**
- Stay tuned for **more** heavy flavour results from ATLAS **in the near future!**

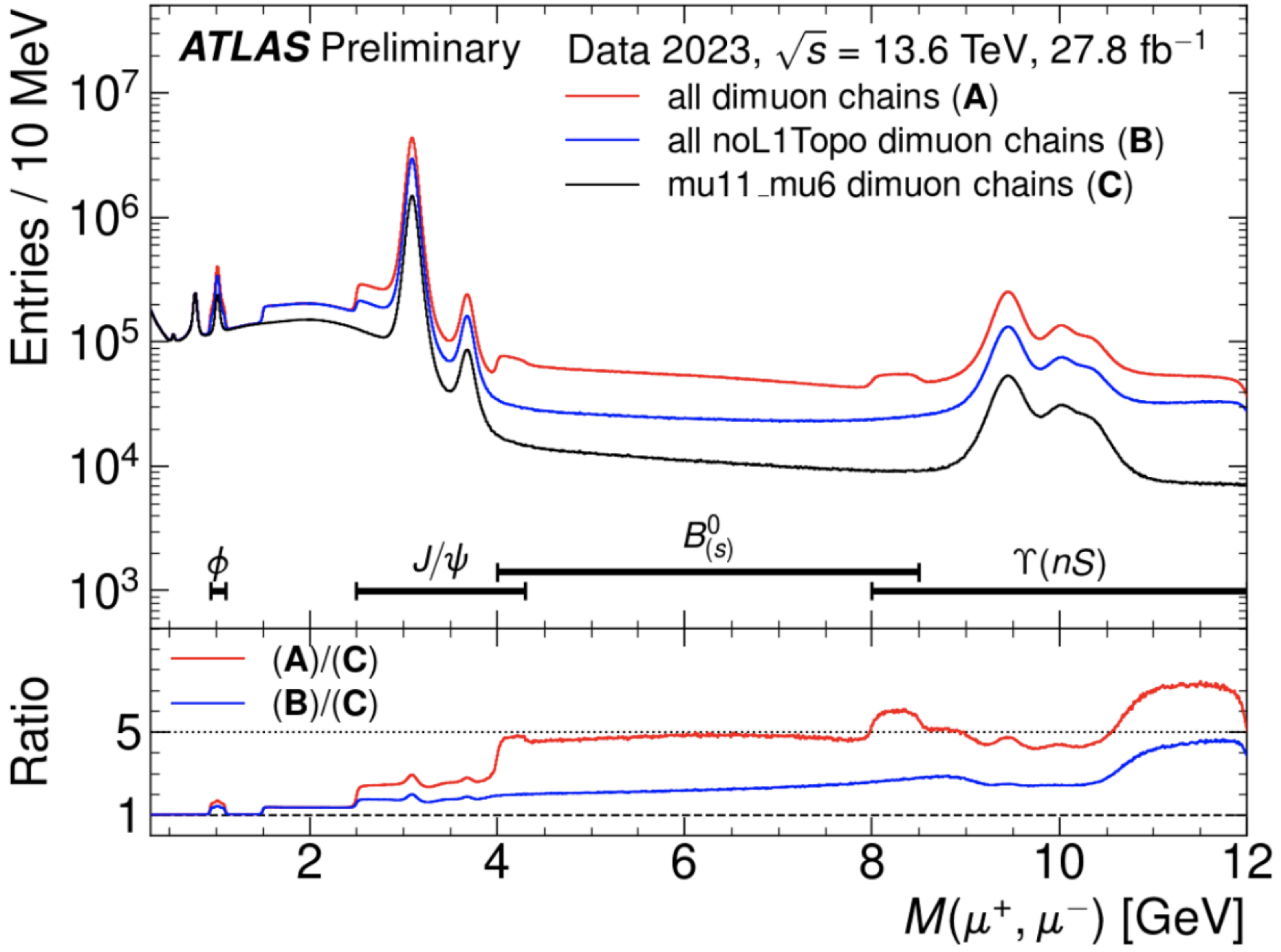

Backup

The ATLAS Detector

- Located around one of the four interaction points at the Large Hadron Collider at CERN
- **General purpose** hermetic detector, capable of measuring many **different particle physics phenomena**, including heavy flavour physics
- Consists of an **Inner Detector** (ID), **Calorimeters** and a **Muon Spectrometer** (MS)
- Particularly relevant for B-physics measurements are the ID and MS
    - ID allows **precise reconstruction of charged tracks** for $|\eta| < 2.5$
    - MS further improves **muon reconstruction and triggering** on muons, covers $|\eta| < 2.7$

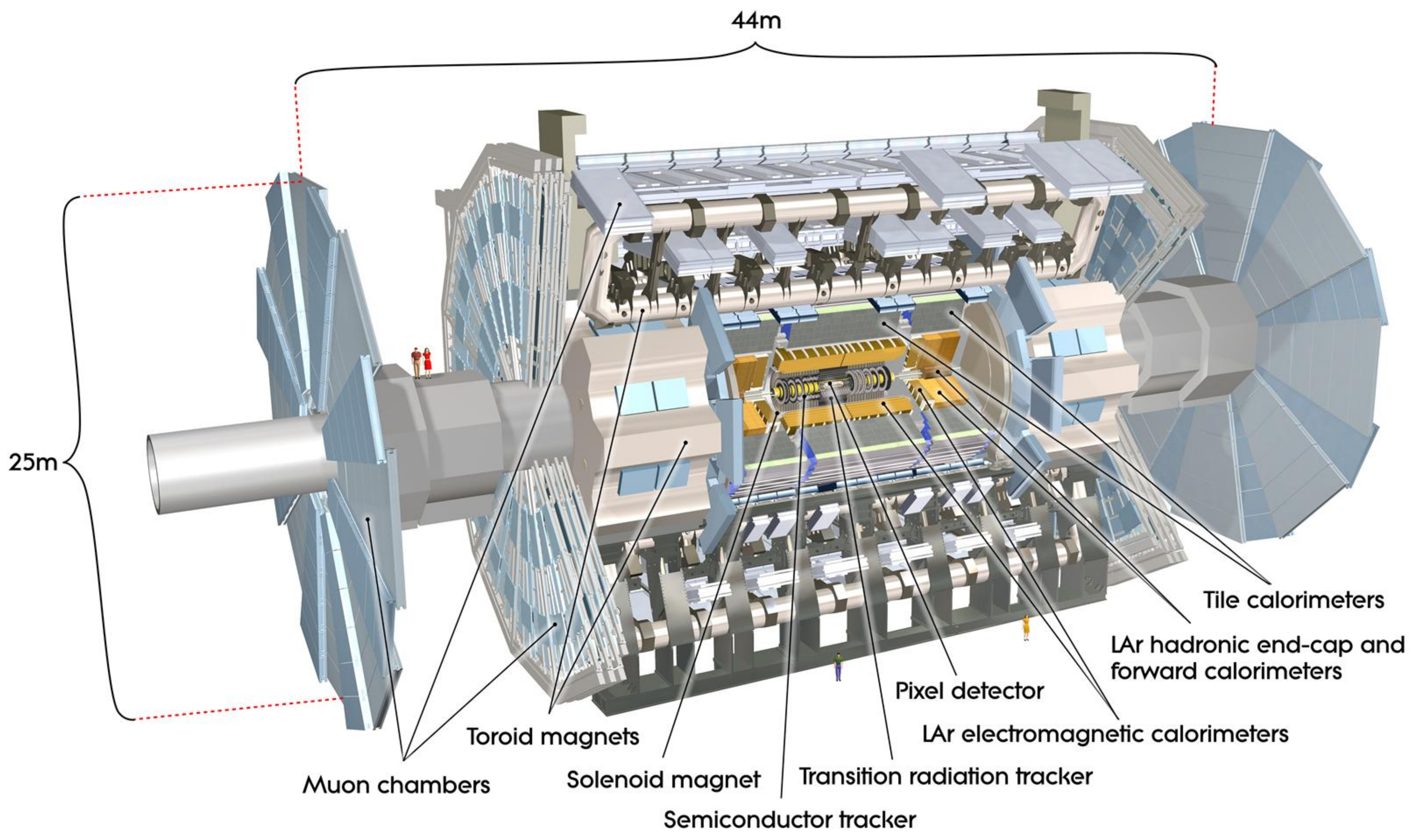

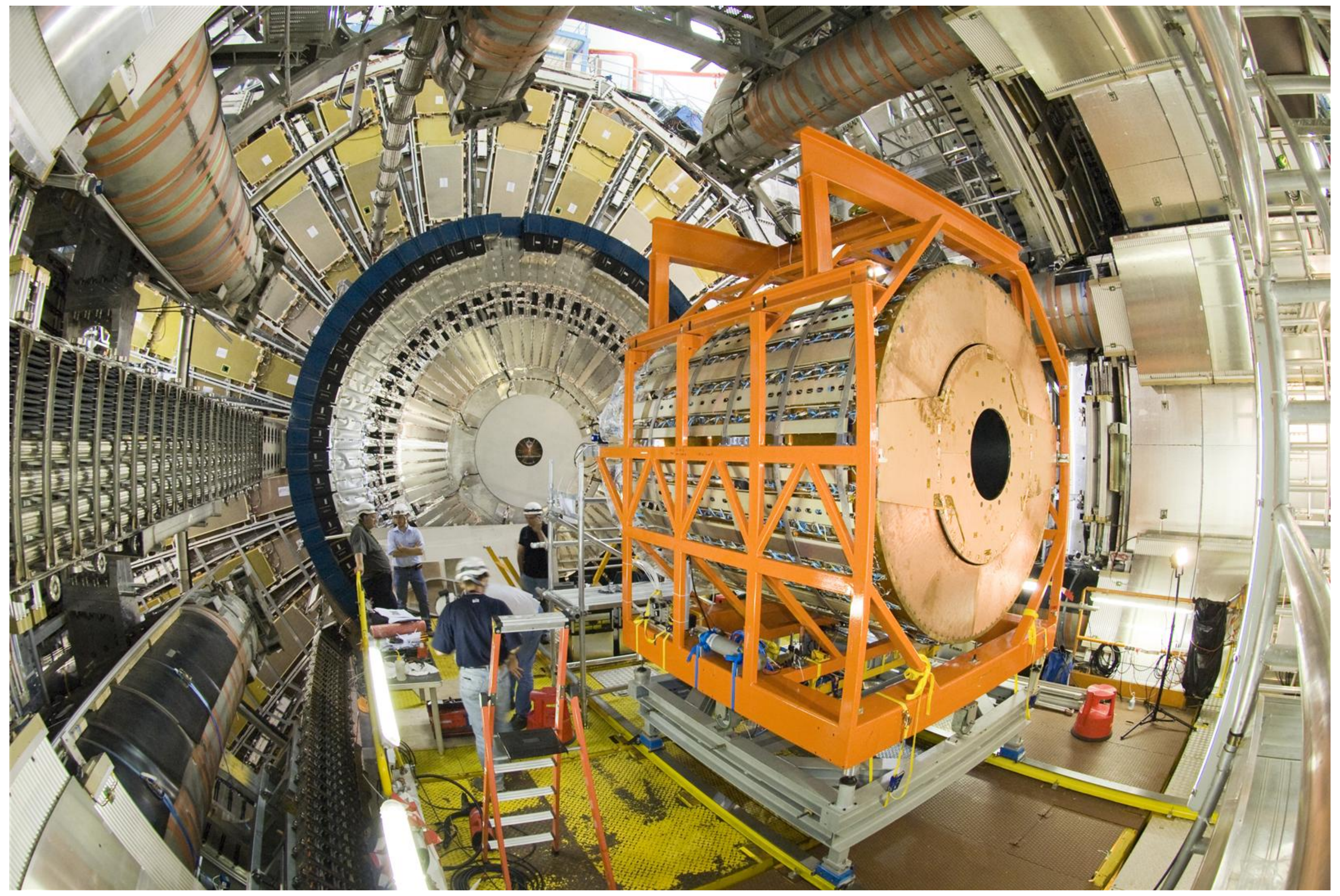

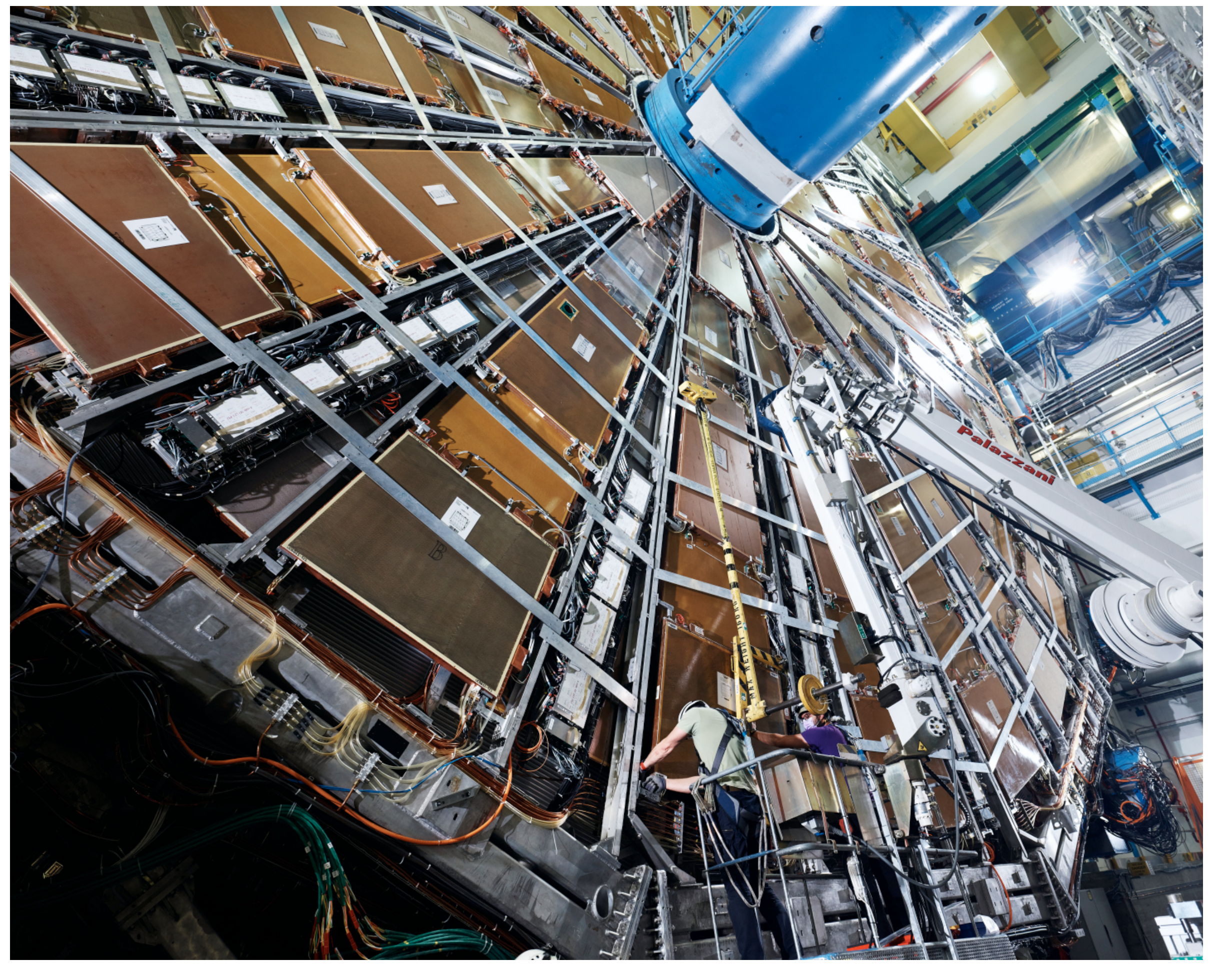

B^0 Lifetime -> Decay Width

The B^0 lifetime τ_{B^0} is related to the decay width Γ_d via

$$\tau_{B^0} = \frac{1}{\Gamma_d}\frac{1}{1-y^2}\left(\frac{1+2Ay+y^2}{1+Ay}\right)$$

Where $\Gamma_d = (\Gamma_L + \Gamma_H)/2$ is the average decay width of the light and heavy mass eigenstates, $y = (\Gamma_L - \Gamma_H)/(2\Gamma_d)$ and $A = \frac{R_H^f - R_L^f}{R_H^f + R_L^f}$ in which R_L^f and R_H^f are defined via the summed decay rate of the $B^0 - \bar{B}^0$ system to final state f:

$$\langle\Gamma(B^0(t))\rangle = \Gamma(B^0(t)) + \Gamma(\bar{B}^0(t)) = R_H^f \text{exp}(-\Gamma_H t) + R_L^f \text{exp}(-\Gamma_L t)$$

Using external inputs for y and A (from HFLAV 2021) it is possible to measure Γ_d from τ_{B^0}

B_d^0 Lifetime 2D Conditional Probability distributions

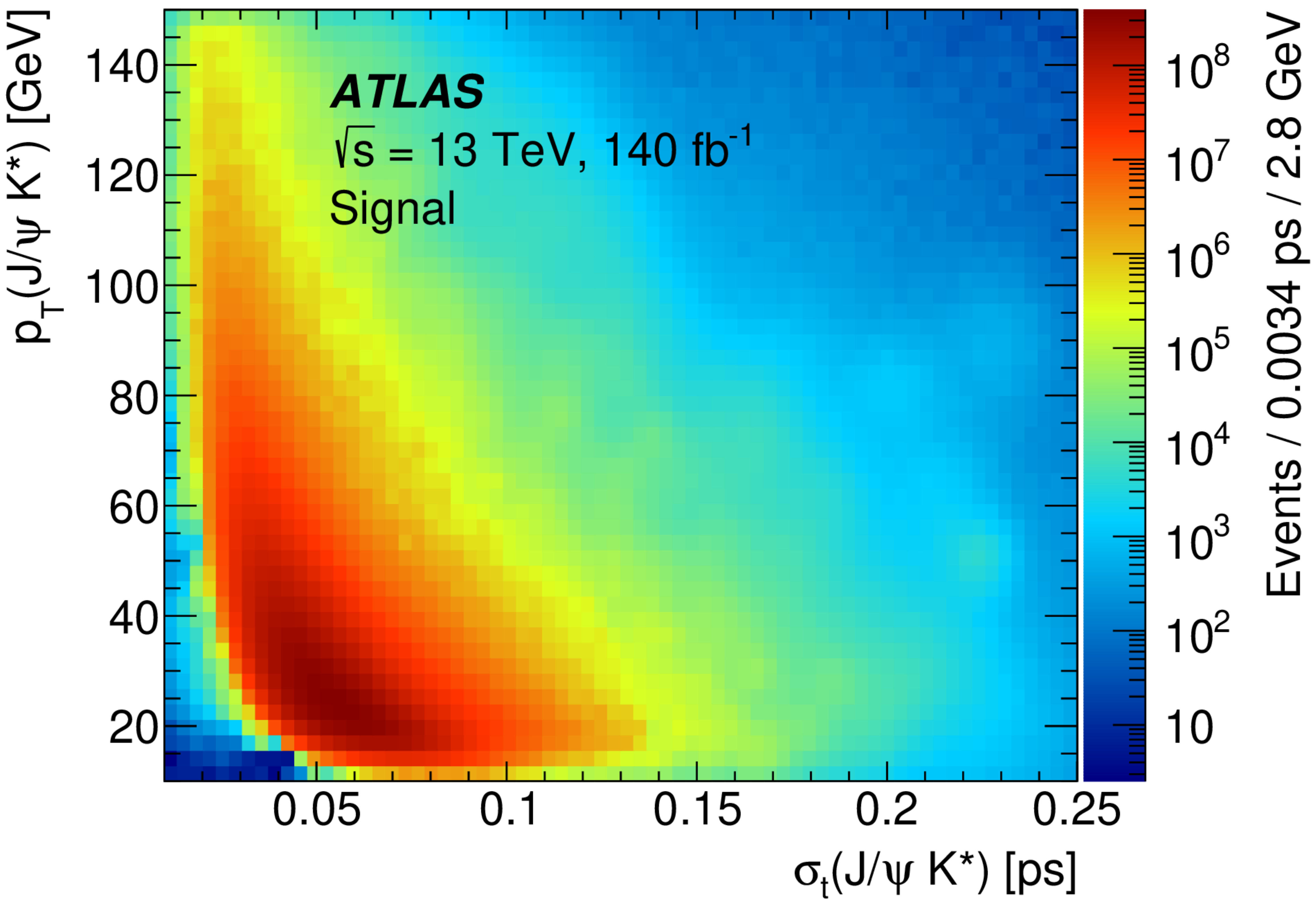

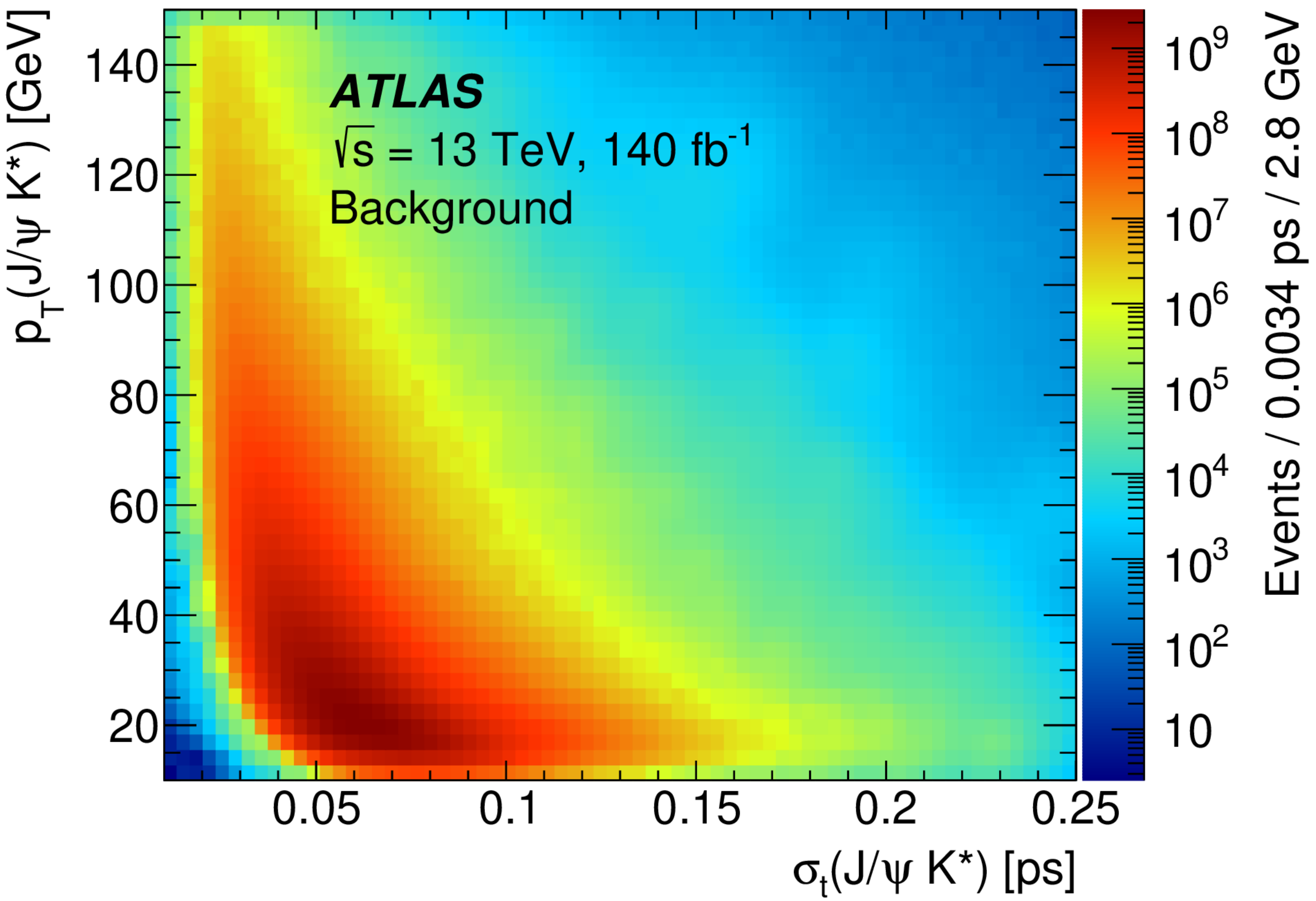

B_d^0 Lifetime Invariant Mass Model

4.1 The invariant mass PDFs

The $\mathcal{M}_{\text{sig}}$ and $\mathcal{M}_{\text{bkg}}$ PDFs model the B^0 signal and background mass shapes, respectively, in the fitted mass range. For the signal, the mass is modelled with a Johnson S_U-distribution [47]:

$$\mathcal{M}_{\text{sig}}(m_i) = \frac{\delta}{\lambda\sqrt{2\pi}\sqrt{1+\left(\frac{m_i-\mu}{\lambda}\right)^2}} \exp\left[-\frac{1}{2}\left(\gamma + \delta \sinh^{-1}\left(\frac{m_i-\mu}{\lambda}\right)\right)^2\right],$$

where μ, γ, δ and λ are free parameters. For the background, the mass distribution is modelled by the sum of a polynomial and a sigmoid function:

$$\mathcal{M}_{\text{bkg}}(m_i) = f_{\text{poly}}(1 + p_0 \cdot m_i) + (1 - f_{\text{poly}})\left(1 - \frac{s(m_i - m_0)}{\sqrt{1 + (s(m_i - m_0))^2}}\right), \quad (3)$$

B_d^0 Lifetime Decay Time Model

The signal proper decay time distribution of the B^0 signal candidates is modelled as an exponential function

$$P_{\text{sig}}(t_i|\sigma_{t_i}, p_{\text{T}_i}) = E(t', \tau_{B^0}) \otimes R(t' - t_i, \sigma_{t_i}),$$

where $E(t, \tau_{B^0}) = (1/\tau_{B^0}) \exp(-t/\tau_{B^0})$ for $t \geq 0$, with the parameter τ_{B^0} standing for the B^0 lifetime.

The proper decay time PDF for the background candidates, P_{bkg}, consists of two parts. One part accounts for the prompt background and consists of the resolution function R only. The other part accounts for the combinatorial background and consists of a sum of three exponential functions, each convolved with the resolution function R. In summary, the background proper decay time PDF takes the form:

$$P_{\text{bkg}}(t_i|\sigma_{t_i}, p_{\text{T}_i}) = \left(f_{\text{prompt}} \cdot \delta_{\text{Dirac}}(t') + (1 - f_{\text{prompt}}) \sum_{k=1}^{3} b_k \prod_{l=1}^{k-1} (1 - b_l) E(t', \tau_{\text{bkg}_k}) \right) \otimes R(t' - t_i, \sigma_{t_i}). \tag{5}$$

Here the τ_{bkg_j} are different lifetimes describing three components of the combinatorial background; the parameters b_j are the relative fractions of these three background components, and f_{prompt} is the prompt component's fraction. Parameters τ_{bkg_j}, f_{prompt} and two of the b_j are free in the fit; $b_3 \equiv 1$ by definition.

B_d^0 Lifetime Conditional Probability Distributions - 1D projections

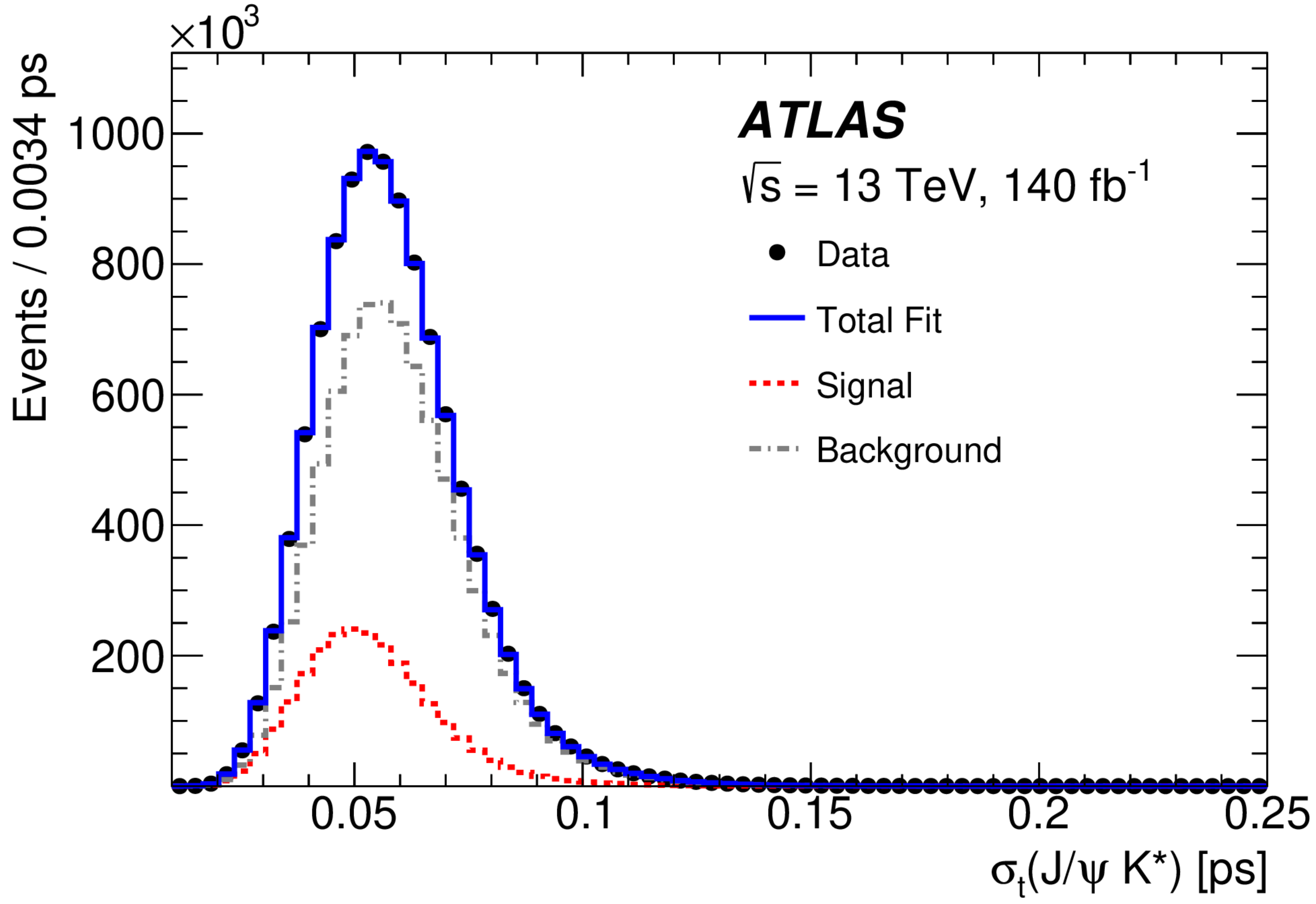

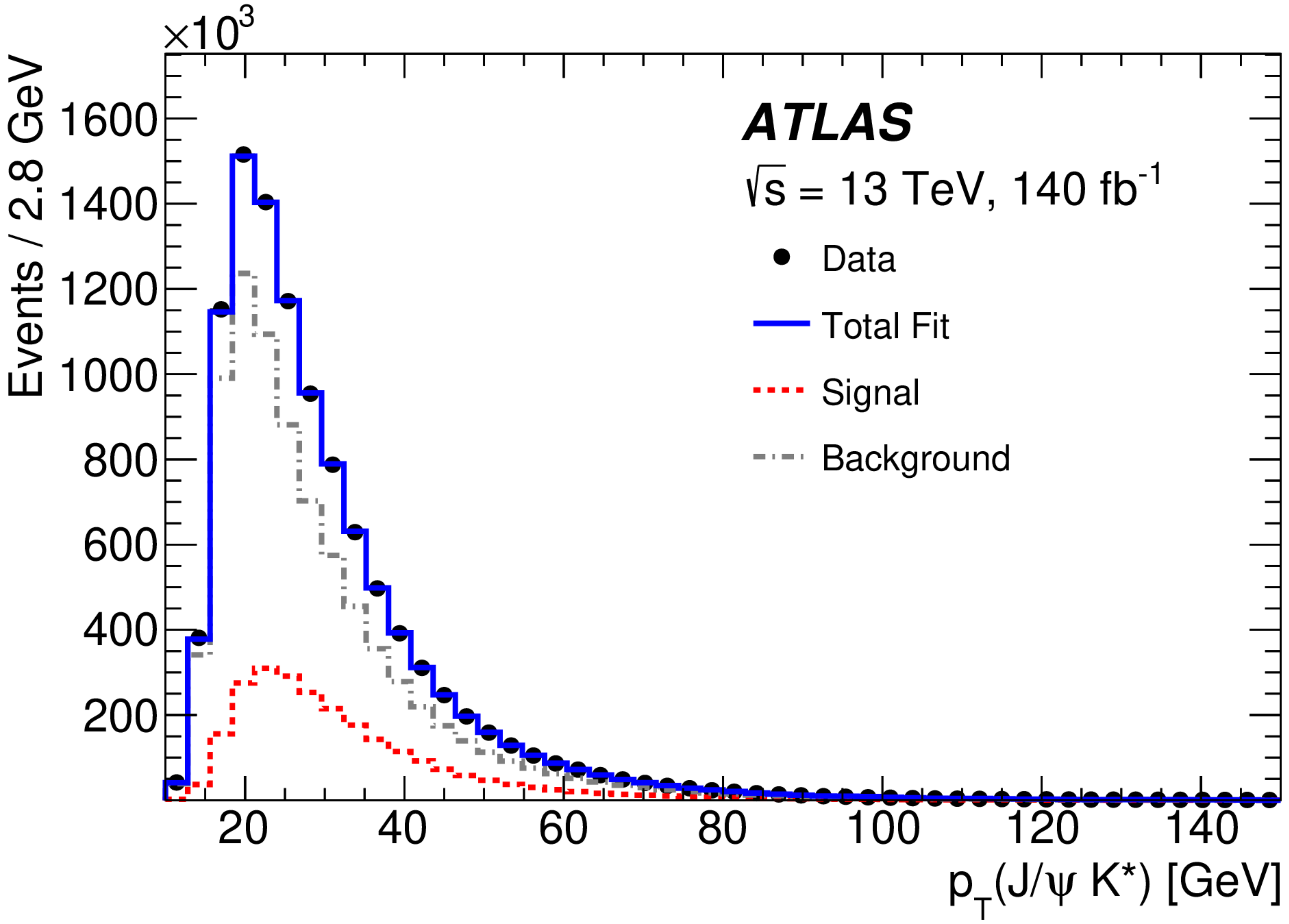

B_d^0 Lifetime Time Efficiency Functions

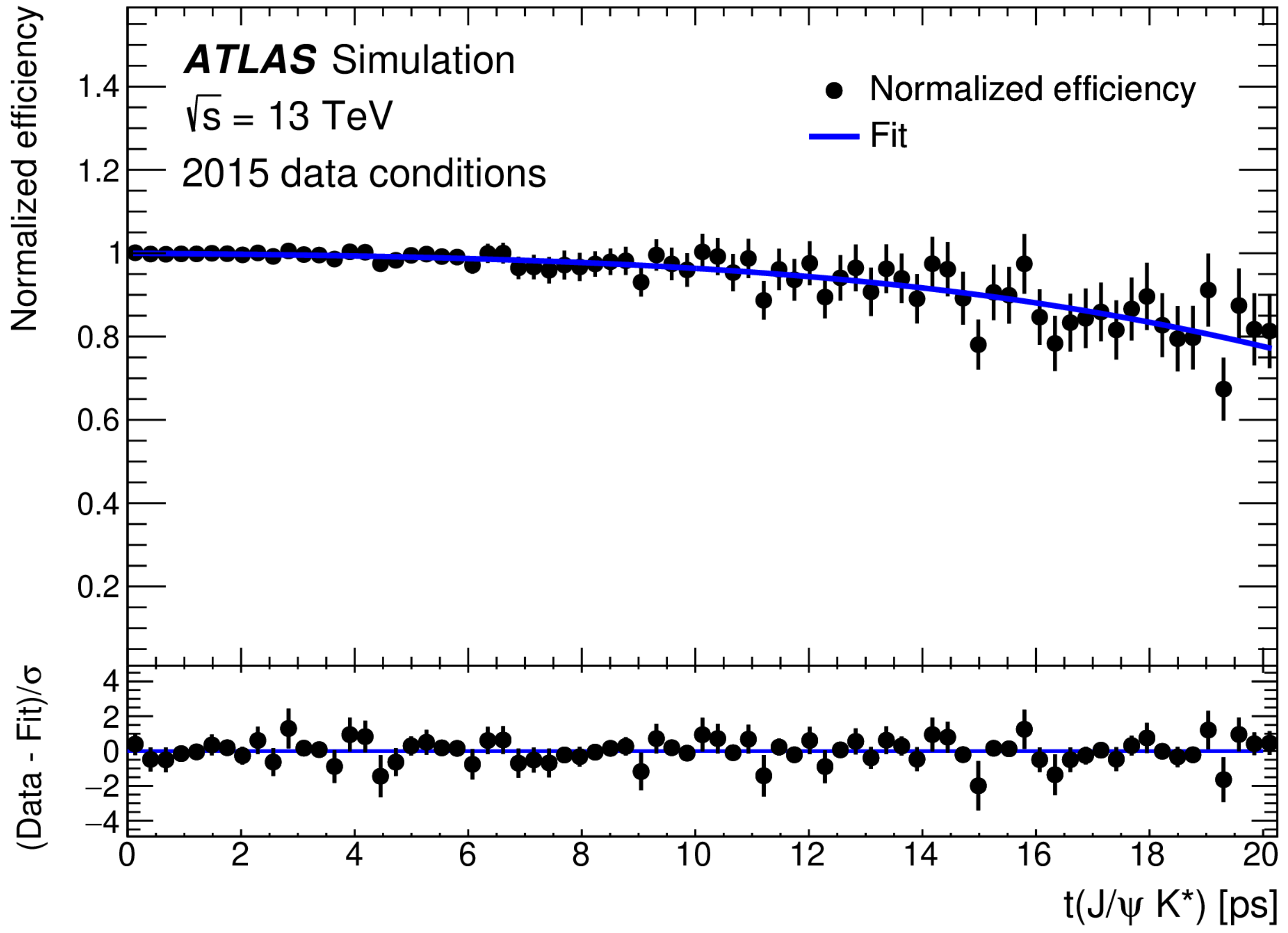

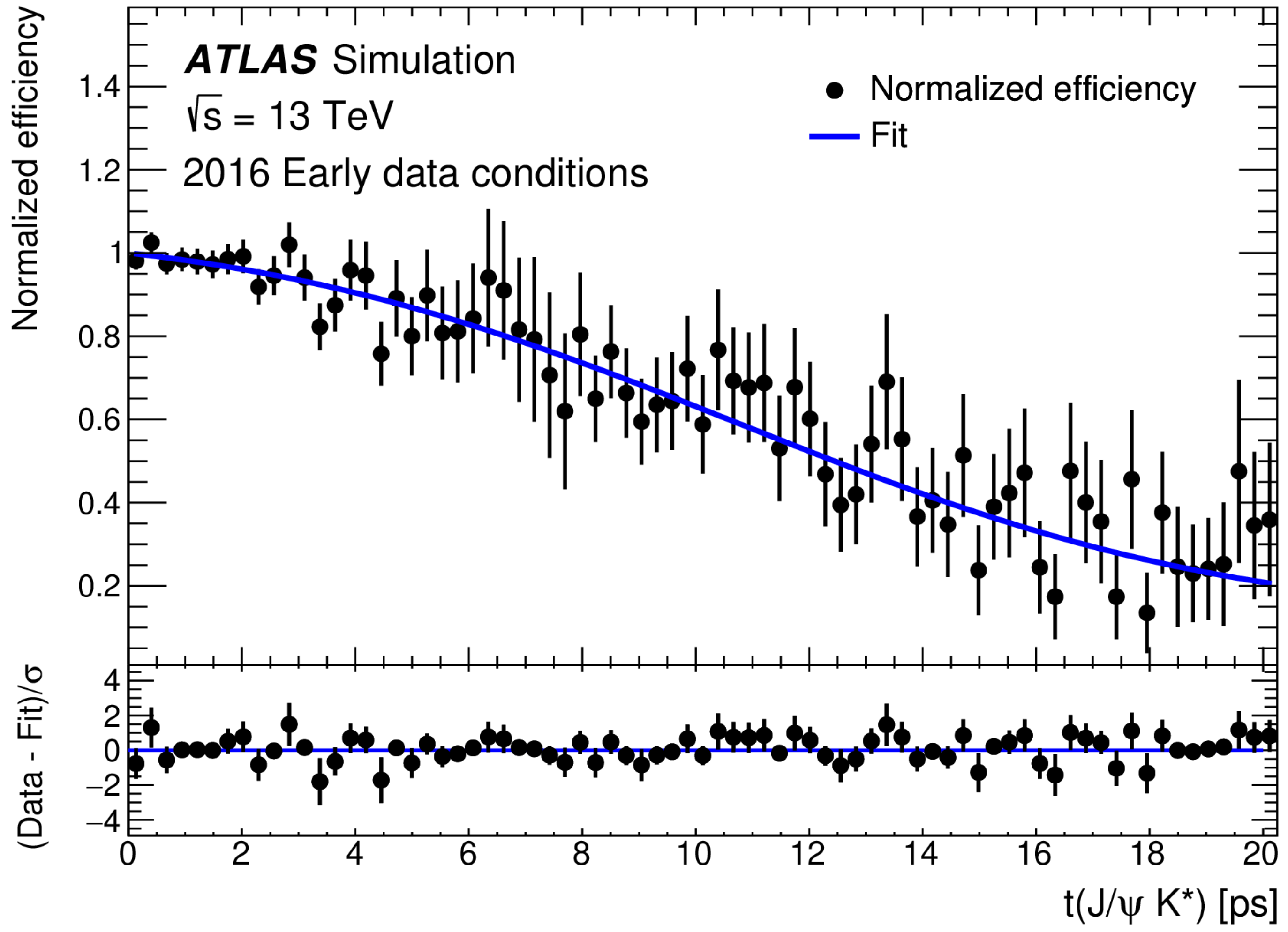

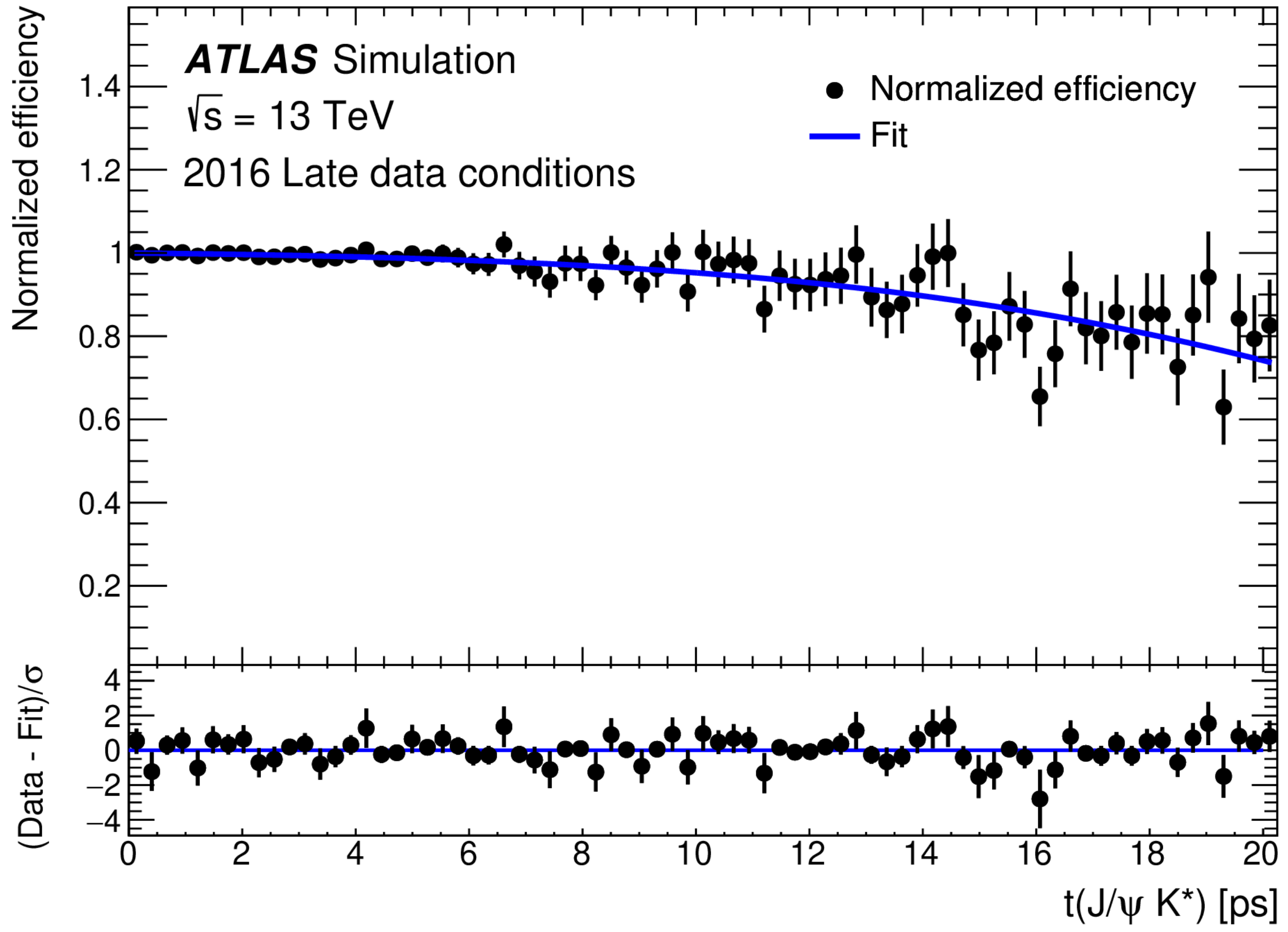

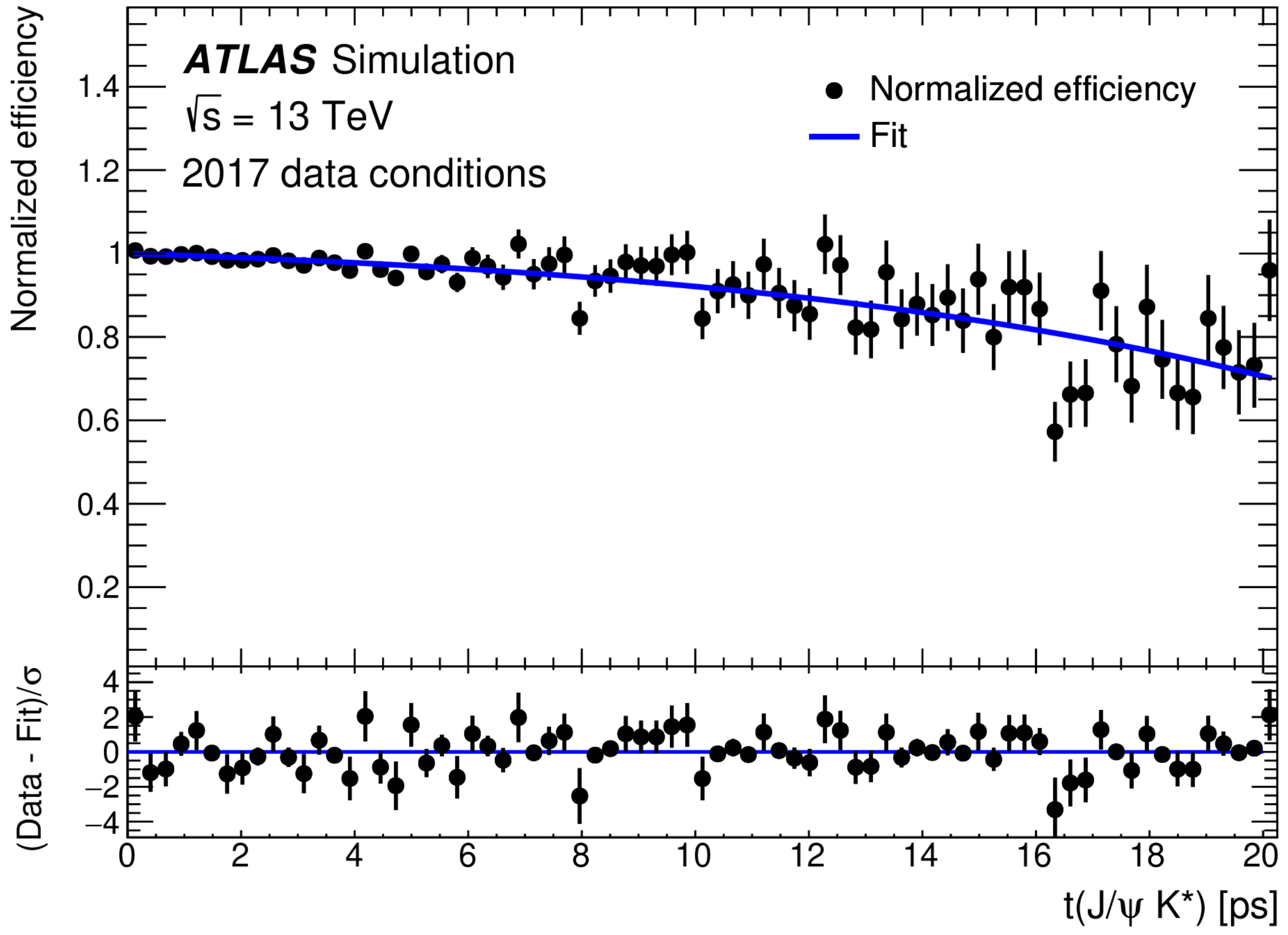

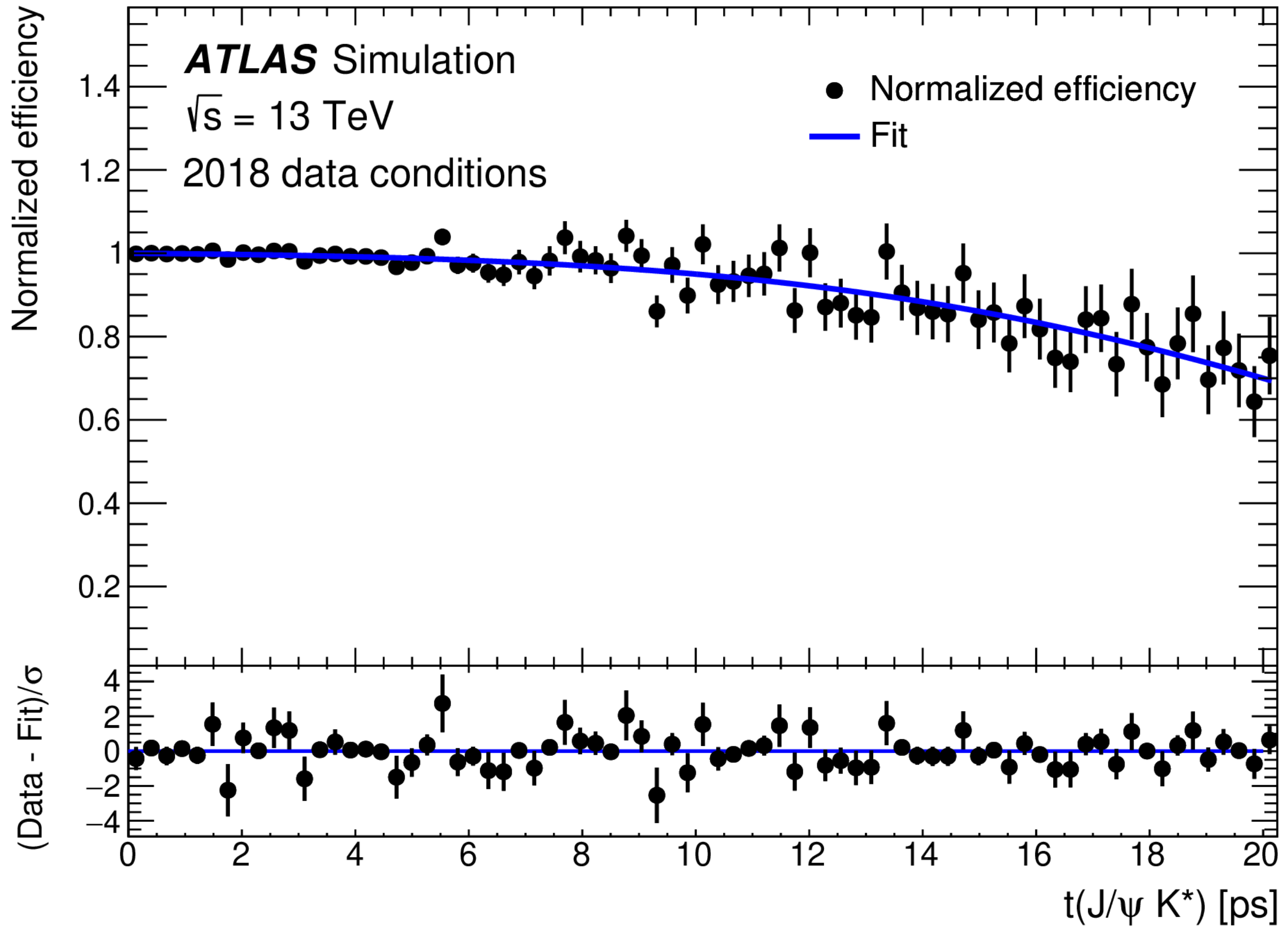

Triggers and offline tracking impose upper limit on transverse impact parameter on the muons/ J/ψ vertex - consequently see inefficiency at large values of decay time

B_d^0 Lifetime stability

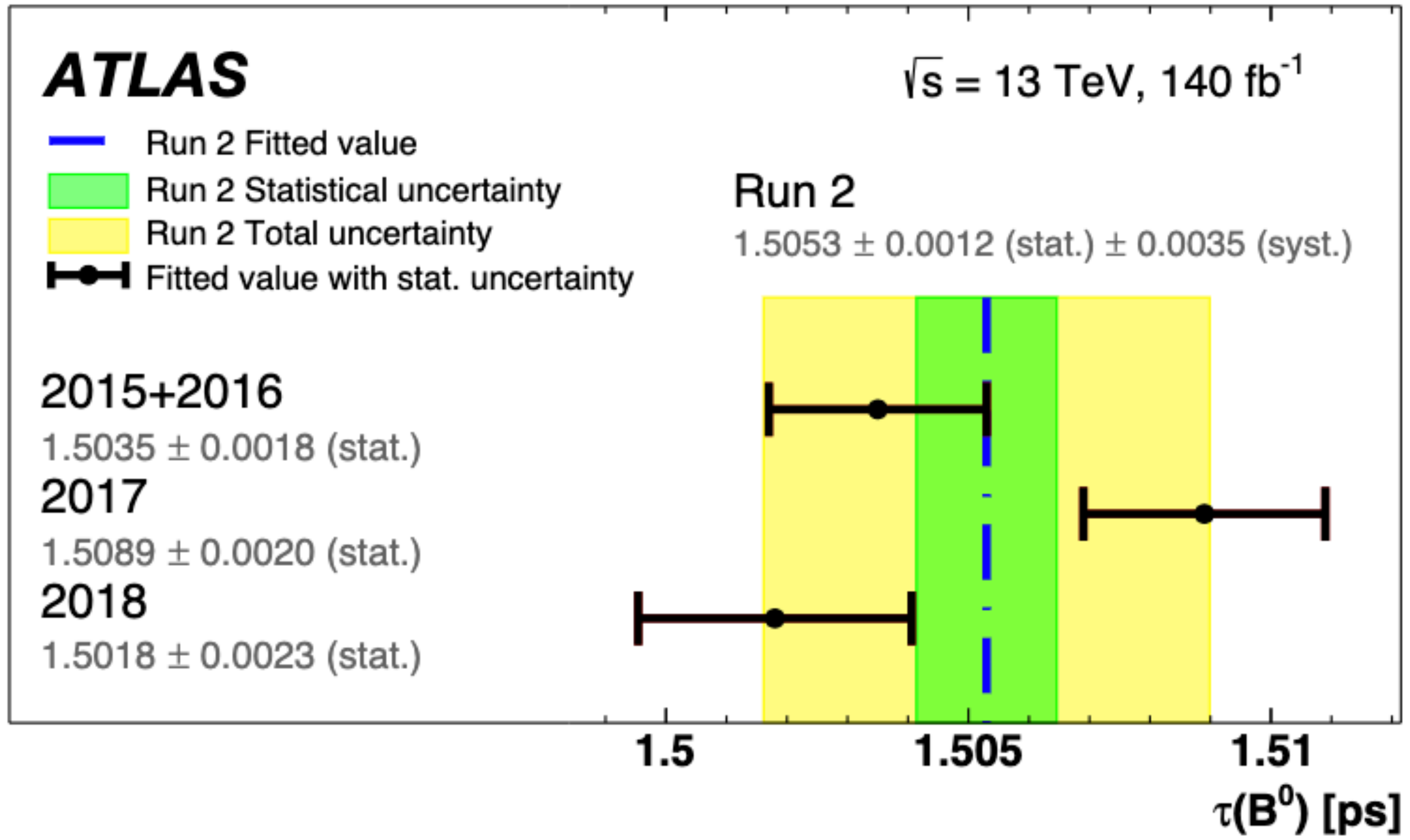

Figure 2: The fitted values of the B^0 lifetime, measured with $B^0 \to J/\psi K^{*0}$ decays, for the 2015+2016, 2017 and 2018 subsamples compared to the value for the whole sample. The B^0 lifetime value for each subsample is shown by a black point, with the error bar indicating the statistical uncertainty.

B_d^0 Lifetime Event Display

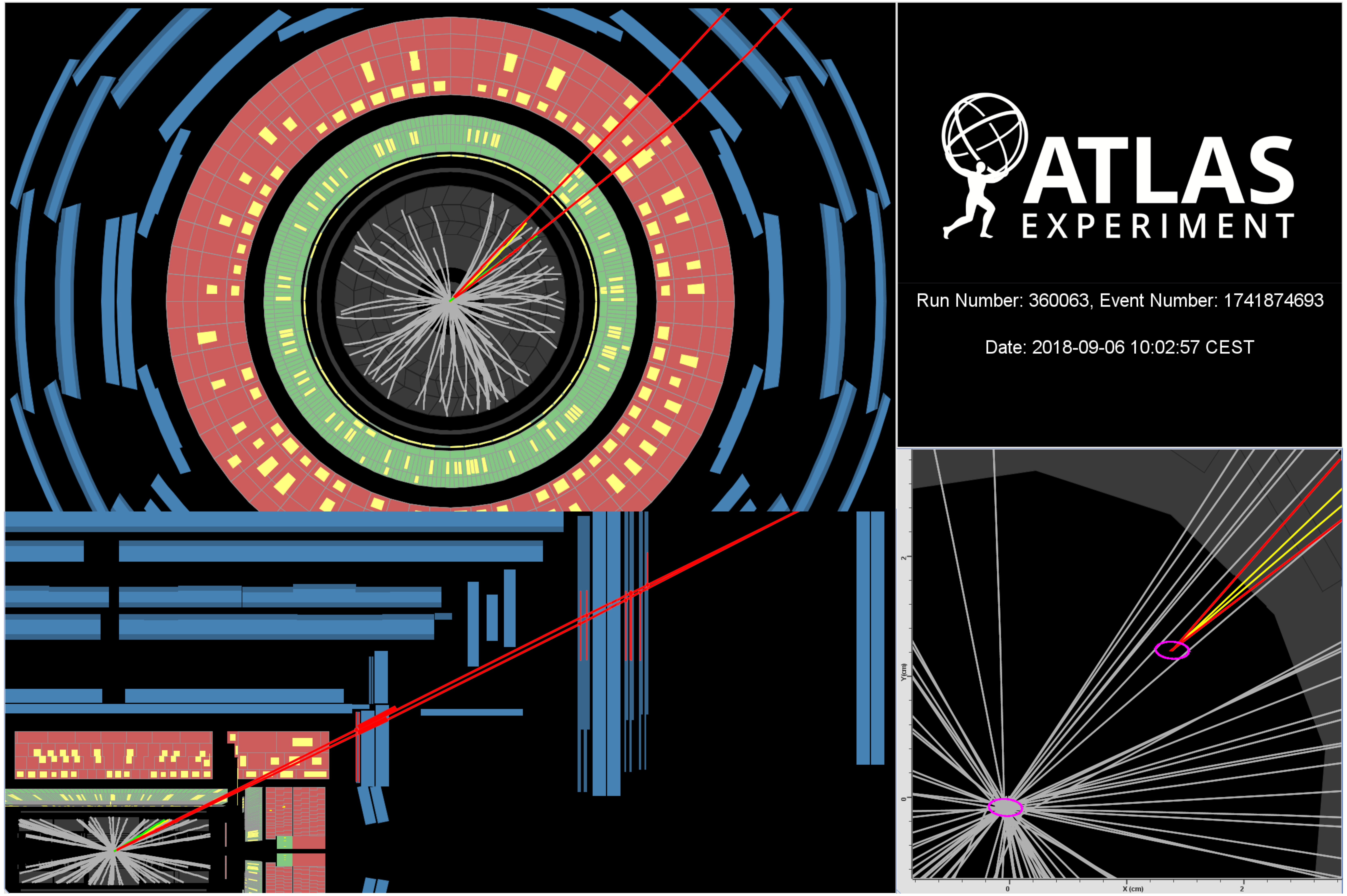

$D^{\pm}$ and $D_s^{\pm}$ cross-sections normalised distributions

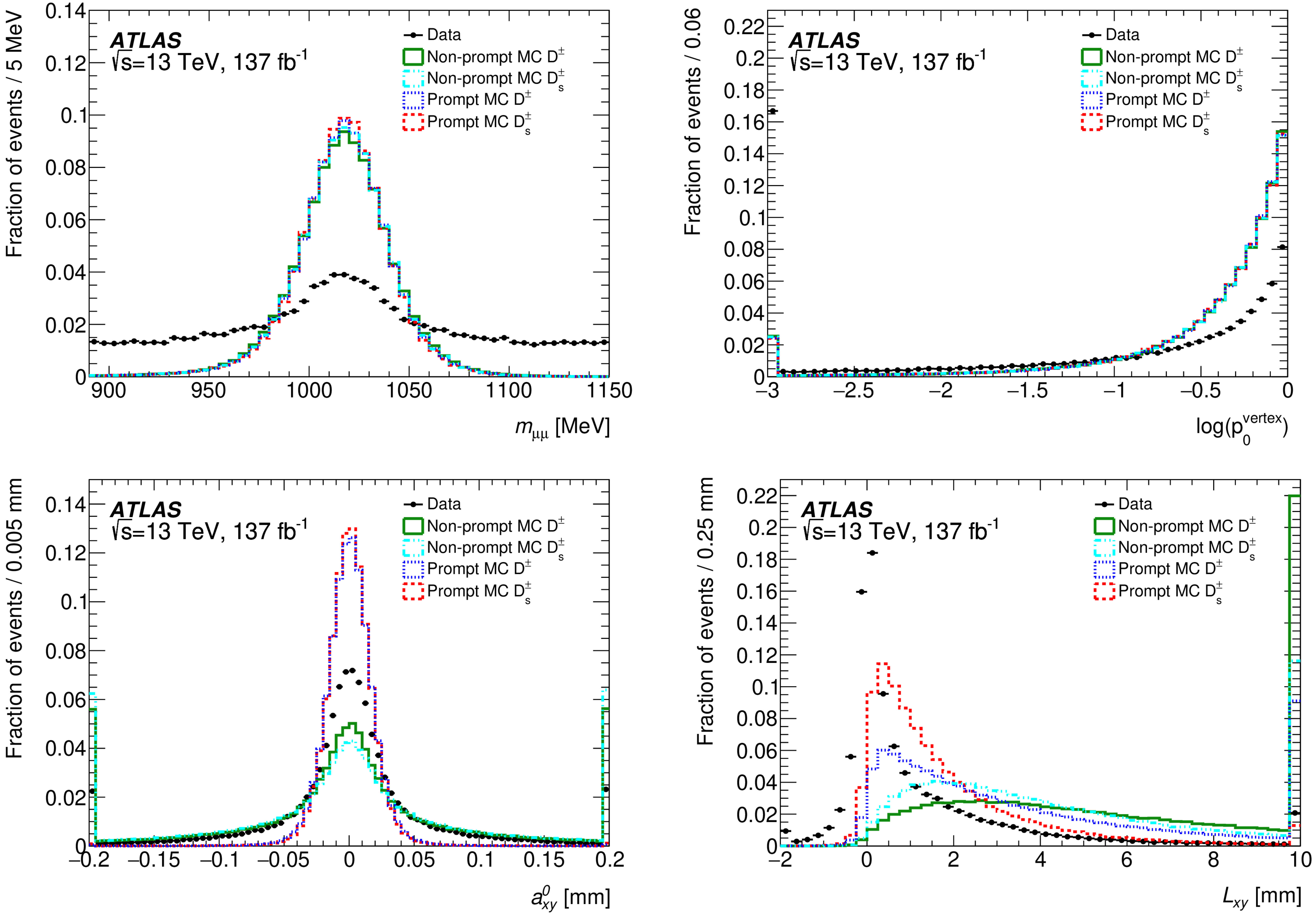

$D^{\pm}$ and $D_s^{\pm}$ cross-sections lifetime fits

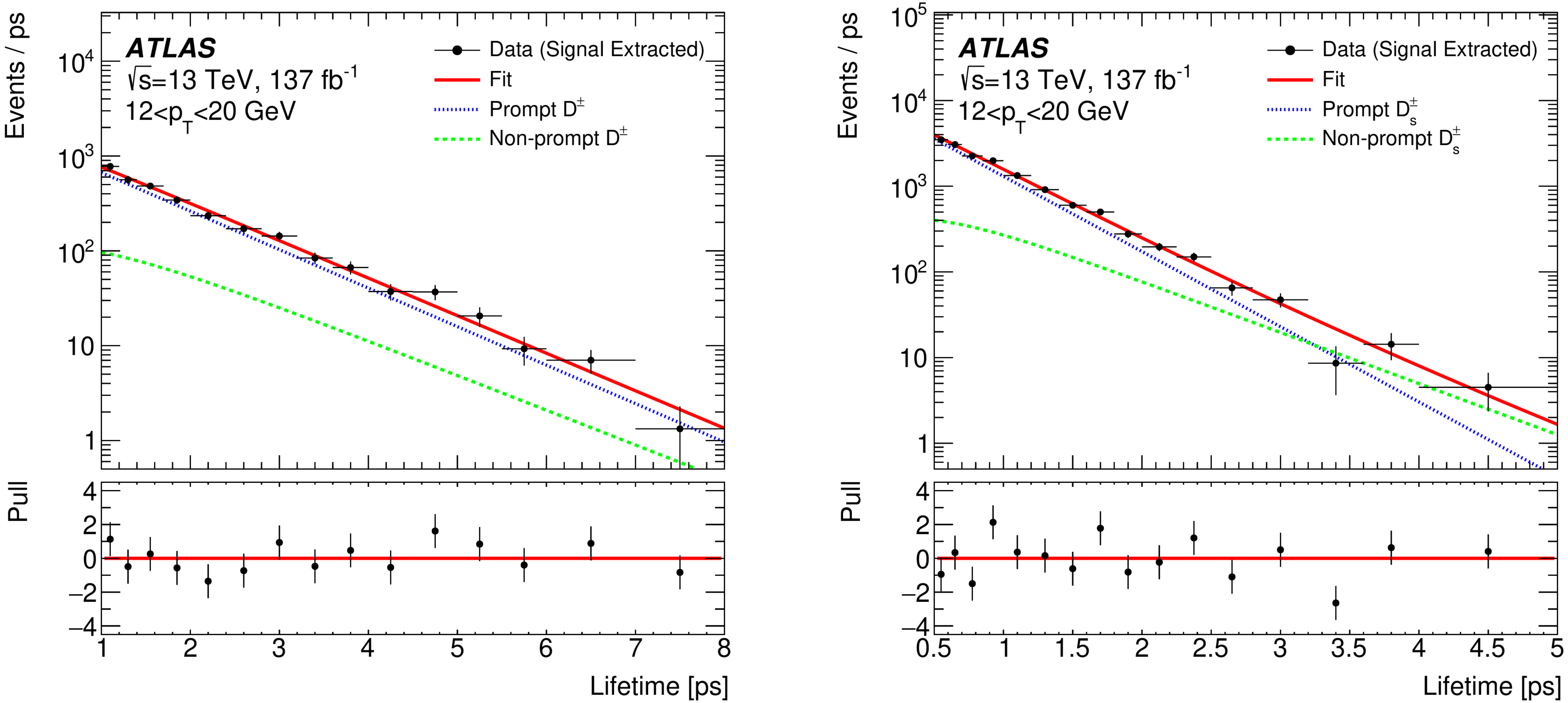

$D^{\pm}$ and $D_s^{\pm}$ systematic uncertainties

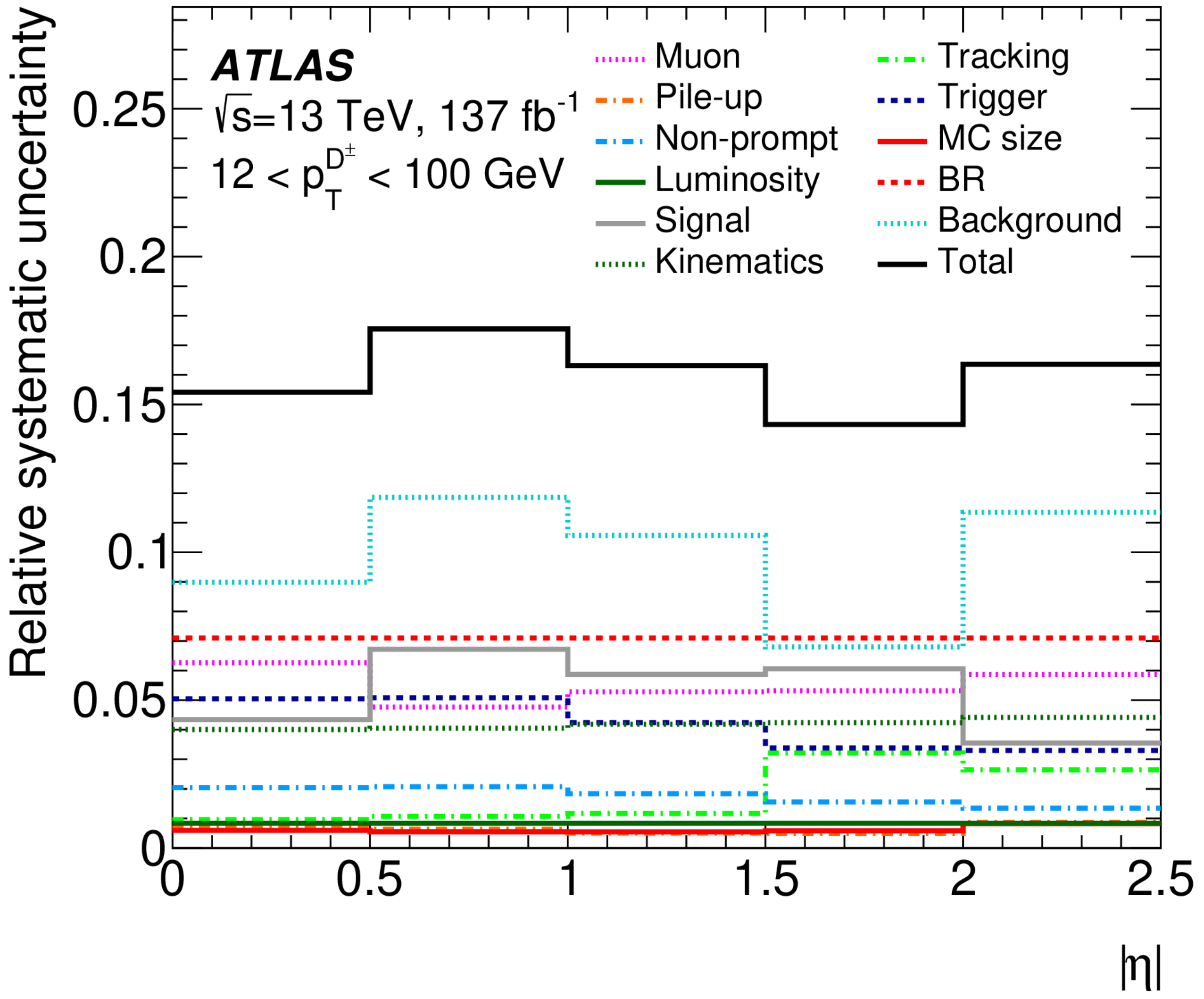

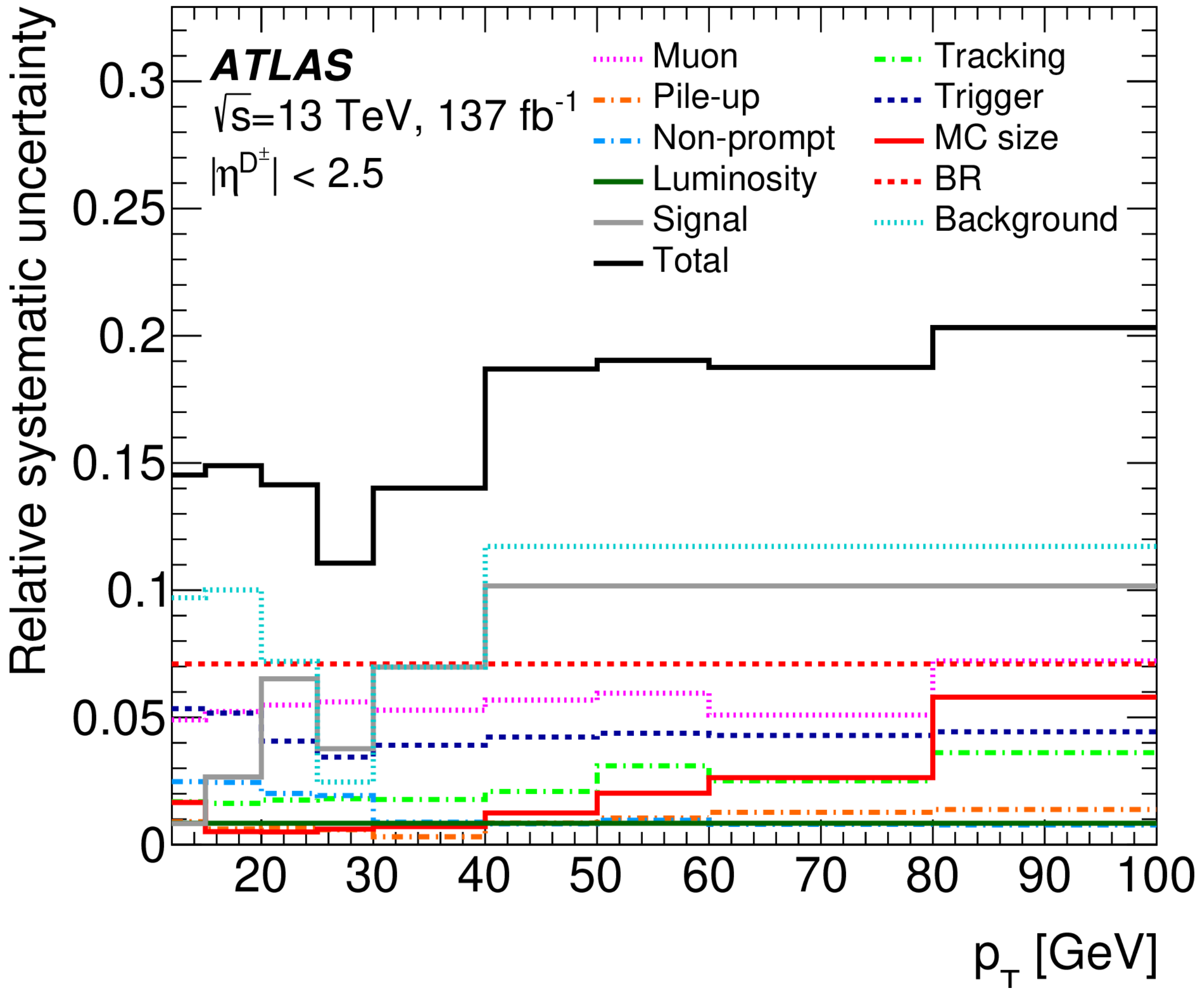

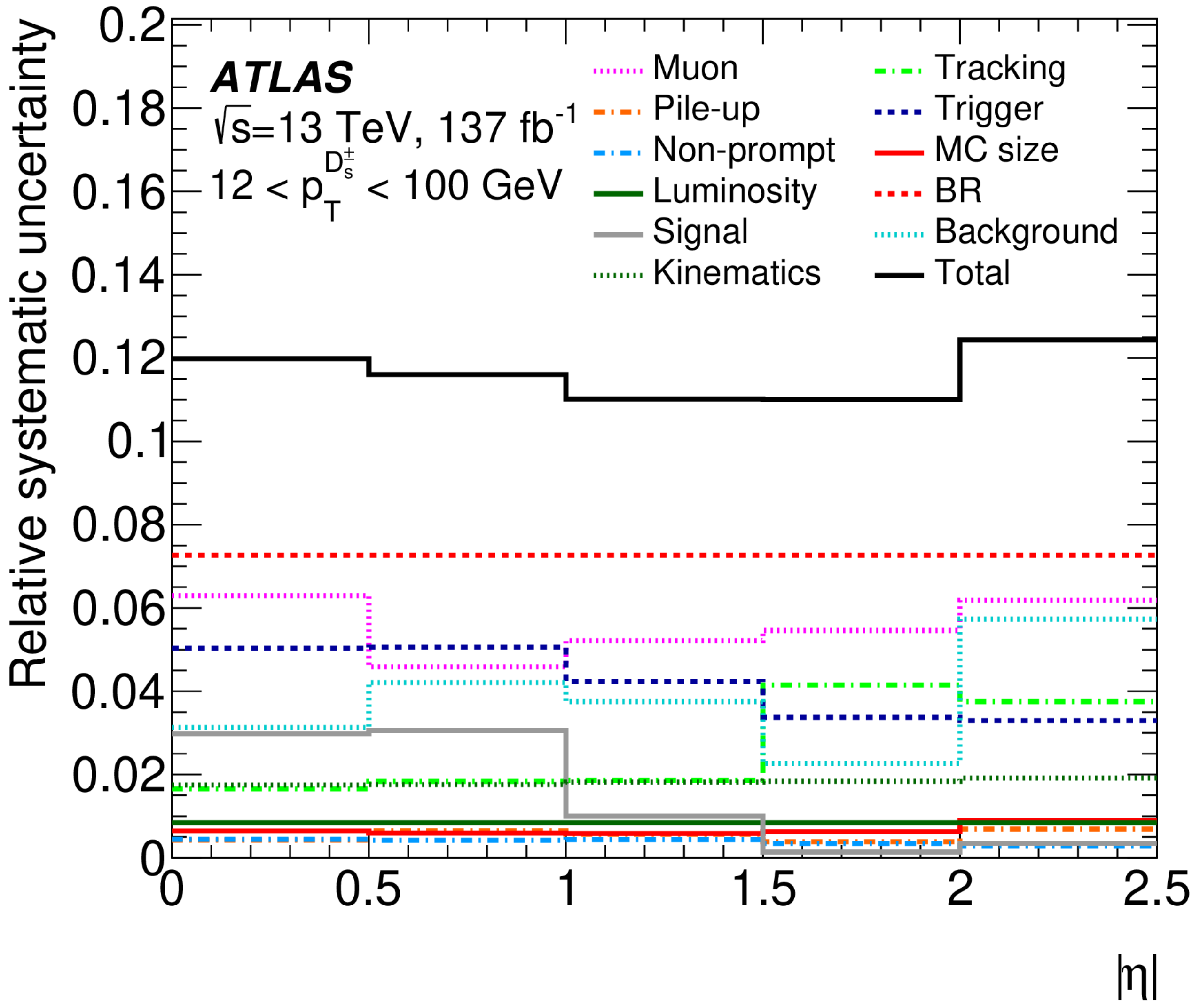

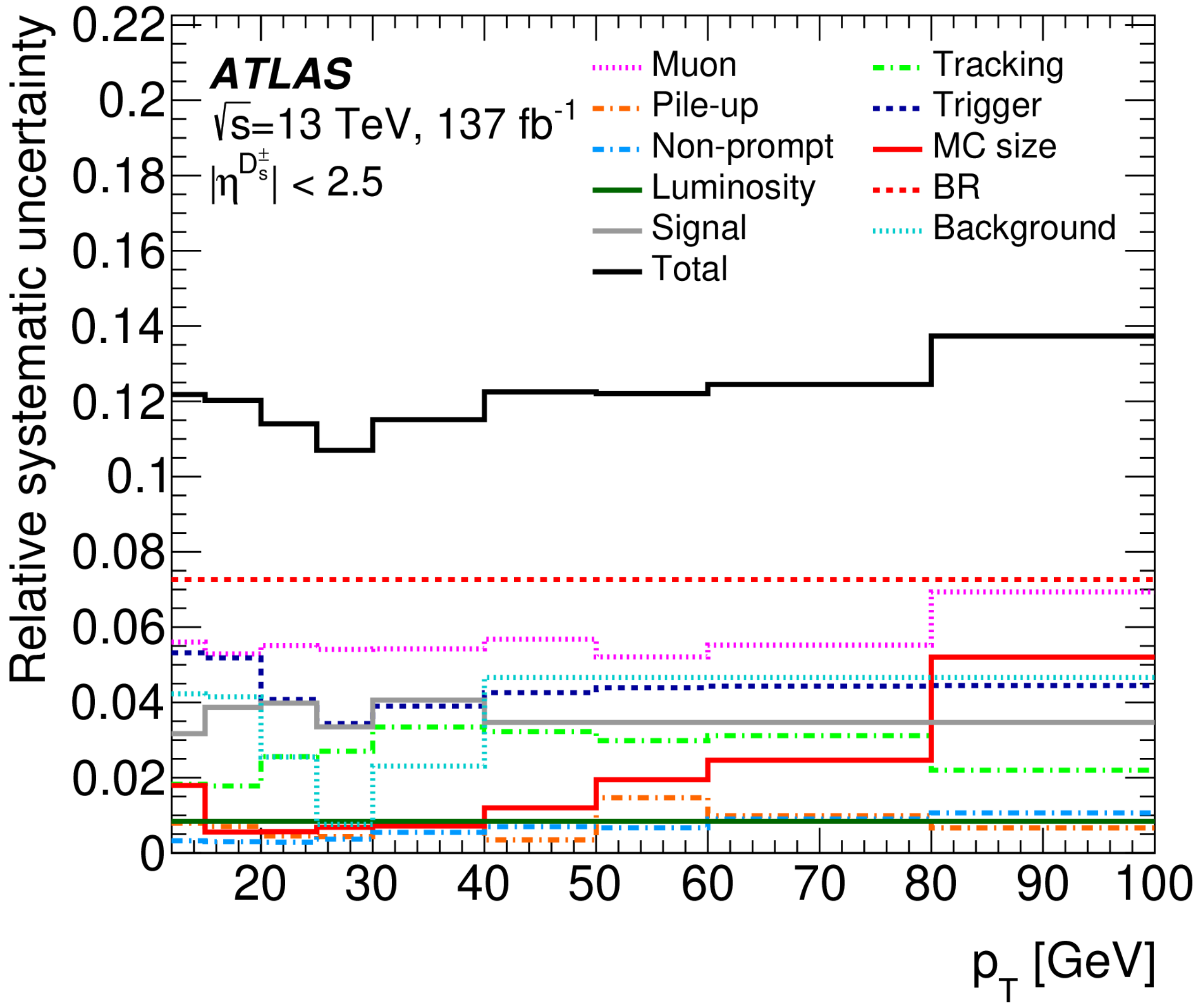

$D^{\pm}$ and $D_s^{\pm}$ cross-sections non-prompt fractions

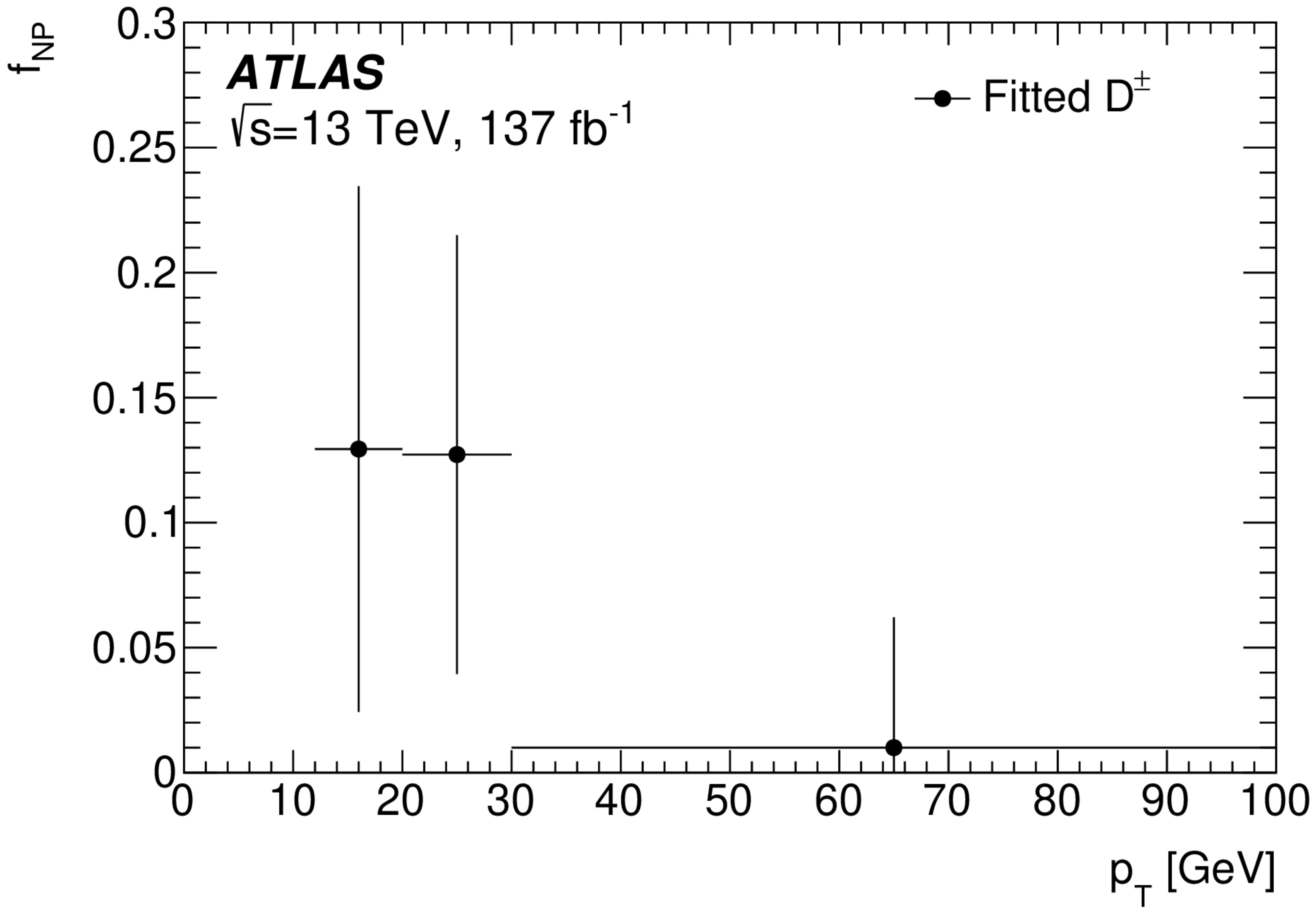

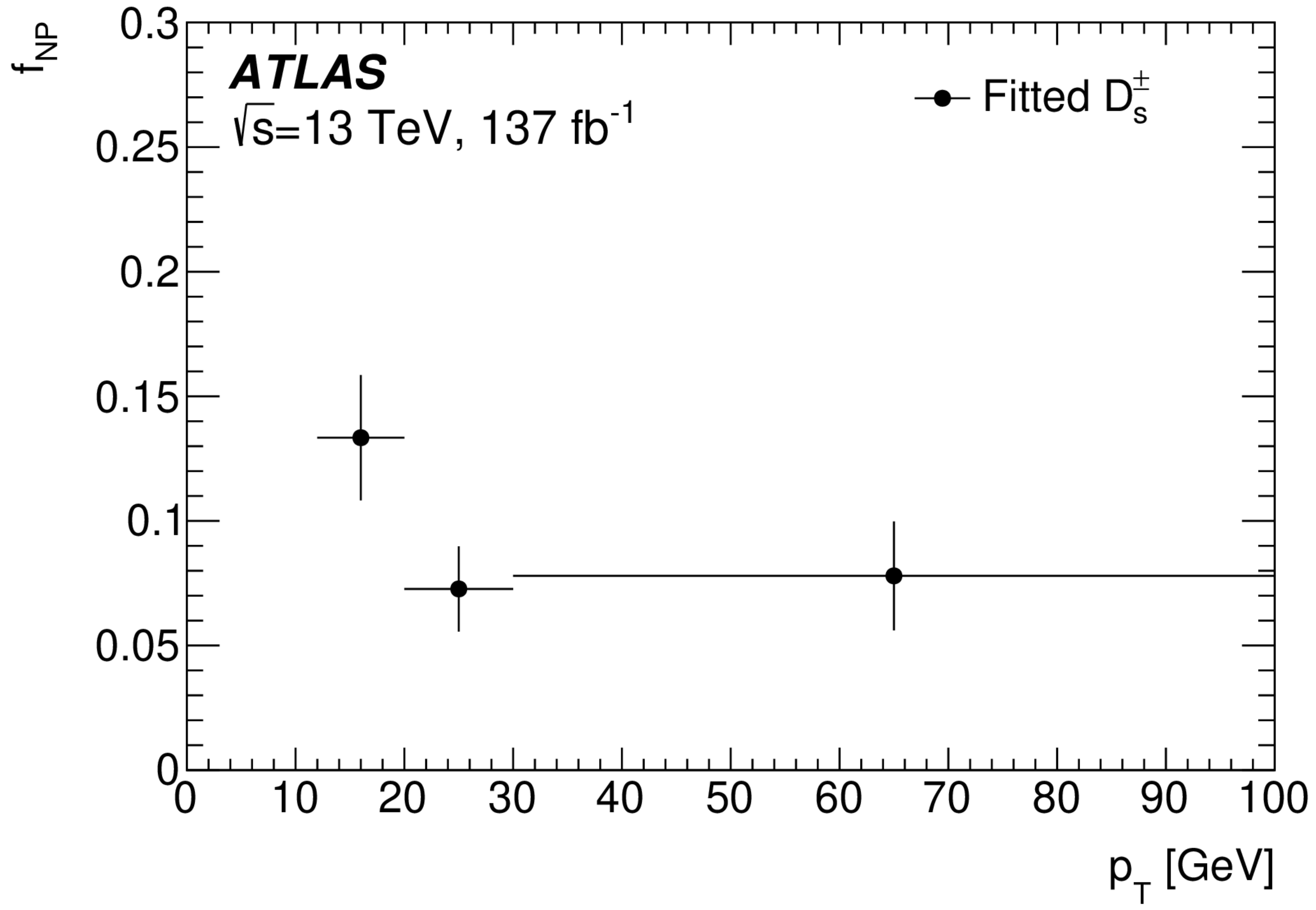

Only statistical Uncertainties shown

Cross-section Extraction

- Differential cross-sections are obtained from the fitted yields through:

$$\left.\frac{\mathrm{d}\sigma}{\mathrm{d}p_{\mathrm{T}}}\right|_i = \frac{S^i_{D^\pm/D_s^\pm}}{\int \mathcal{L}\mathrm{d}t \times C^i \times \mathcal{B}(D^\pm/D_s^\pm \to \phi(\mu\mu)\pi^\pm) \times \Delta^i p_{\mathrm{T}}},$$

$$\left.\frac{\mathrm{d}\sigma}{\mathrm{d}|\eta|}\right|_j = \frac{S^j_{D^\pm/D_s^\pm}}{\int \mathcal{L}\mathrm{d}t \times C^j \times \mathcal{B}(D^\pm/D_s^\pm \to \phi(\mu\mu)\pi^\pm) \times \Delta^j |\eta|},$$

- Where C_i are correct for the acceptance, reconstruction and efficiency of the analysis selections

$$\mathcal{B}(D_s^\pm \to \phi(\mu\mu)\pi^\pm) = \frac{\mathcal{B}(D_s^\pm \to \phi(K^+K^-)\pi^\pm)}{\mathcal{B}(\phi \to K^+K^-)} \times \mathcal{B}(\phi \to \mu\mu),$$